

Numerical Simulation of Two-phase Separation in T-junction

by

Low Huei Ming

12637

Dissertation submitted in partial fulfillment of

The requirements for the

Bachelor of Engineering (Hons)

(Mechanical Engineering)

MAY 2013

Universiti Teknologi PETRONAS
Bandar Seri Iskandar
31750 Tronoh
Perak Darul Ridzuan

CERTIFICATION OF APPROVAL

Numerical Simulation of Two-phase Separation in T-junction

by

Low Huei Ming

A project dissertation submitted to the
Mechanical Engineering Programme
Universiti Teknologi PETRONAS
in partial fulfillment of the requirement for the
BACHELOR OF ENGINEERING (Hons)
(MECHANICAL ENGINEERING)

Approved by,

(Dr. William Pao)

UNIVERSITI TEKNOLOGI PETRONAS

TRONOH, PERAK

May 2013

CERTIFICATION OF ORIGINALITY

This is to certify that I am responsible for the work submitted in this project, that the original work is my own except as specified in the references and acknowledgements, and that the original work contained herein have not been undertaken or done by unspecified sources or persons.

LOW HUEI MING

ABSTRACT

T-junctions are commonly used in distributing two-phase flow by piping networks especially in oil and gas industries. However, the nature splitting of liquid-gas phases is a major challenge and is complicated due to the large number of variables that influence it. Understanding the behavior of two-phase flow through a T-junction is very essential as it has significant impact on oil and gas transportation pipeline networks, operation and control of process and power industries and lastly the maintenance efficiency of all the components downstream from the junction. This paper provides a detailed analysis on the effect of associated variables on phase separation efficiency in T-junction. Hence, the analysis uses and develops a numerical model for simulation of two-phase flow distribution in T-junction to elucidate an in depth understanding on two-phase separation at different operating conditions and parameters. In order to achieve the objective, the developed model consists of horizontal main arm and vertical side arm while CFD method is employed to simulate the fluid flow. The present study identifies that the overall mass split ratio, the initial gas saturation and gas density are the most influential factors on fraction of gas taken off in T-junction. Subsequently, the effect of inclination angle of gravity on flow split is investigated and it does not play a significant role on phase separation. At the end of this project, the phenomenon of phase maldistribution when a two-phase mixture passes through a T-junctions is well understood and hence the underlying potential as a simple, cost saving, passive partial separator is able to be included in the design of pipeline networks in the petroleum industry.

ACKNOWLEDGEMENT

My completion of Final Year Project will not be a success without many peoples. Hereby, I would like to acknowledge my heartfelt gratitude to those I honor.

First of all, I would like to thank my direct supervisor, Dr. William Pao, senior lecturer of Mechanical Engineering Department, Universiti Teknologi PETRONAS. Thanks to his precious supervision, guidance, support, assistance and opportunities throughout my project. Apart from the technical aspects, he is also provides valuable guidance on my personal development.

Subsequently, I would like to thank my friends who are giving me suggestions and comments on my work for further improvements. Last but not least, I would like to thank my family members for their support during my final year study. With their support, I managed to perform well for my final year of undergraduate study.

Table of Contents

ABSTRACT.....	i
ACKNOWLEDGEMENT.....	ii
CHAPTER 1: INTRODUCTION	
1.1 Project Background.....	1
1.2 Problem Statement	2
1.3 Objectives.....	2
1.4 Scope of Study	3
CHAPTER 2: LITERATURE REVIEW	
2.1 Flow patterns	4
2.2 Flow pattern identification	7
2.3 Influence of dominant forces on separation efficiency in a T-junction....	10
2.4 Effect of variation diameter ratio on two-phase split in T-junction and mitigation of phase splitting	11
2.5 Effect of inclined branched arm on flow splitting behavior in T-junction.....	13
2.6 The approaches of two-phase flow split prediction.....	14
2.7 Basic theory of separation efficiency in T-junction.....	16
2.8 Related governing equations for gas-liquid flow in T-junction.....	17
CHAPTER 3: METHODOLOGY	
3.1 Development of model simulation	19
3.2 Mesh dependency check analysis.....	21
3.3 Project activities	26
3.4 Gantt Chart and Key Milestone.....	27

3.5	Tools required	28	
CHAPTER 4: RESULTS AND DISCUSSIONS			
4.1	Verification of the Simulation Model with Experiment data.....	29	
4.2	Parametric studies on two-phase separation efficiency in T-junction.....	32	
4.3	Concluding Remarks	41	
CHAPTER 5: CONCLUSION AND RECOMMENDATIONS			44
LIST OF FIGURES.			iii
LIST OF TABLES			iv
REFERENCES			46

LIST OF FIGURES

Figure 1.1: Diagram of a T-junction

Figure 2.1: Two-phase flow patterns in vertical pipes

Figure 2.2: Two-phase flow patterns in horizontal flows

Figure 2.3: X-ray absorption probability density functions of void fractions

Figure 2.4: Electrode configurations for conductance method

Figure 2.5: Layout of process tomography applications

Figure 3.1: Schematic T-junction with applied inlet and outlets boundary conditions

Figure 3.2: Computational mesh refinement of T-junction

Figure 3.3: Pressure convergence versus mesh density

Figure 3.4: Pressure contour of mixture phase with total number of 4272 tetrahedral cells and 253919 tetrahedral cells.

Figure 3.5: Velocity contour of water phase with total number of 4272 tetrahedral cells and 253919 tetrahedral cells.

Figure 3.6: Streamlines of air velocity with total number of 4272 tetrahedral cells and 253919 tetrahedral cells.

Figure 3.7: Project Process Flow Chart

Figure 3.8: Five Phases of Project Flow Activities

Figure 4.1: Computational grid of T-junction

Figure 4.2: Simulated flow split curves compared with experimental results

Figure 4.3: Effect of Diameter ratio on Fraction of gas taken off with initial velocity of 15m/s and Methane density of 0.6679kg/m^3

Figure 4.4: Effect of Initial gas saturation on Fraction of gas taken off with initial mixture velocity of 15m/s and Methane density of 0.6679kg/m³

Figure 4.5: Effect of Inclination angle of gravity on Fraction of gas taken off with overall mass split ratio of 0.30, 0.60 and 0.90

Figure 4.6: Effect of Gas density on Fraction of gas taken off with overall mass split ratio of 0.50 and 0.95 with an inlet mixture velocity of 12m/s

Figure 4.7: Effect of Overall mass split ratio on Fraction of gas taken off with initial gas saturation of 0.83 and 0.96 with inlet mixture velocity of 15m/s and methane density of 0.6679kg/m³

Figure 4.8: Parameters' weighting factor on two-phase separation in T-junction

Figure 4.9: Parameters' sensitivity to fraction of gas taken off

LIST OF TABLES

Table 3.1: Input parameters for validations and parametric studies

Table 3.2: Gantt chart and Milestones for FYP I and FYP II

Table 4.1: Fraction of gas taken off per unit change of diameter ratio for mass split ratio, M of 0.3, 0.6 and 0.9

Table 4.2: Fraction of gas taken off per unit change of initial gas saturation for mass split ratio, M of 0.3, 0.6 and 0.9

Table 4.3: Fraction of gas taken off per unit change of inclination angle of gravity for mass split ratio, M of 0.3, 0.6 and 0.9

Table 4.4: Fraction of gas taken off per unit change of gas density for mass split ratio, M of 0.50 and 0.95

Table 4.5: Fraction of gas taken off per unit change of overall mass split ratio for initial gas saturation, S_g of 0.83 and 0.96

CHAPTER 1:

INTRODUCTION

1.1 Project Background

Two-phase flow is the simultaneous flow of two different phases separated from each other by a distinct interface, with at least one of the phases must be a fluid which is either gas or liquid. Basically, there are four types of two-phase flow which are gas-liquid, gas-solid, liquid-liquid and liquid-solid. The most common types of two-phase flow are gas-liquid and liquid-liquid. The most complex flow is gas-liquid since they combine the characteristics of a deformable interface and the compressibility of one of the phases. This flow is also found widely in a whole range of industrial applications. This includes the pipeline or piping system for the transport of oil-gas mixtures.

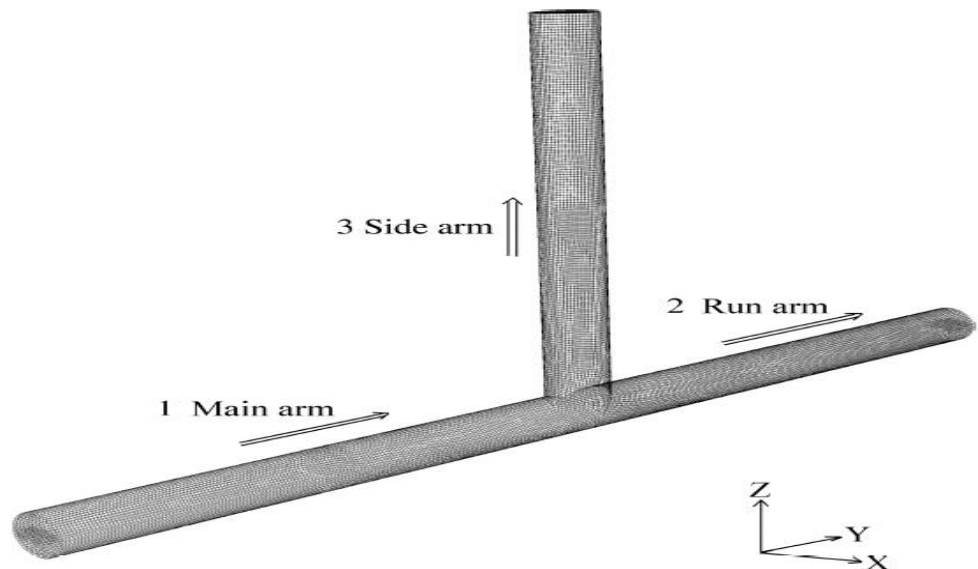


Figure 1.1 Diagram of a T-junction (Liu *et al.*, 2011)

A T-junction consists of three main components which are the main arm, run arm and side arm. When a two-phase mixture flows through a T-junction, the phases tend to separate in different proportions among the outlet arms. The lower density or light phase tends to be preferentially diverted into the side arm, while the heavier phase will flow straight through the run arm. Hence, the side-arm of the branching T-junction will carry a higher proportion of the lighter phase than the run arm.

1.2 Problem Statement

T-junctions are very common within pipe networks in the petroleum industry as they are commonly used to separate the components which are oil, gas and water prior to flow to the place of destination. They are used to replace the tasks of vessel for separation process in piping network due to the requirement of large space and expensive cost. However, the efficiency of the phase separation and the geometry/shape of the T-junction are not well understood. This will lead to significant impact on oil and gas transportation pipeline networks, operation and control of process and power industries and lastly the maintenance efficiency of all the components downstream from the junction. For instance, in gas distribution networks, condensate can be formed in pipelines during winter due to low surrounding temperatures. This was then found that the condensate appears at some delivery stations while the other stations receive only dry gas. This uneven separation may result in creating operational and separation problems in the end.

1.3 Objectives

This project aims to:

- a) To examine the geometric effect on wet methane gas separation efficiency in T-junction.
- b) Analysis of the fraction of gas taken off in a T-junction at different operating conditions and parameters.

1.4 Scope of Study

The main focus of the study is to investigate the wet gas separation efficiency in T-junction at different operating conditions and parameters through simulation of flow. Among the parameters that will be tested include the diameter ratio of inlet arm to side arm, initial gas saturation, working fluids density ratios, overall mass split ratio, inlet mixture velocity and the inclination angle of gravity. These parameters will be analyzed with the scope of circular cross sectional area, horizontal main arm and vertical side arm using water and methane gas as working fluids. Temperature factor will not be included during the simulation modeling since this study is focusing on Newtonian fluids.

CHAPTER 2:

LITERATURE REVIEW

2.1 Flow patterns

There are two main types of flow in pipes which are the vertical flow and horizontal flow.

2.1.1 Vertical flow in pipes

Baker (2003) and Wren (2001) stated that liquid and gas phases distribute themselves into four main patterns for co-current up flow of gas and liquid in vertical pipes.

- **Bubbly flow:** Numerous bubbles are observable as the gas is dispersed in the form of discrete bubbles in the continuous liquid phase. The bubbles travel within the flow and maybe coalescing and they are generally varied in size and shape. According to Serizawa and Kataoka (1988), there are some situations whereby the bubbles congregate mainly at pipe centre which called core-peaking, while the others congregate near the pipe wall which known as wall-peaking. Furthermore, small bubbles flowing at different velocity distribute themselves into two sub-patterns called discrete bubbly and dispersed bubbly flow. Both sub-patterns flow are generated due to lower liquid velocities and high liquid velocities respectively.
- **Slug flow:** It is also known as **plug flow**. It occurs when the bubbles have coalesced and the small bubble size tends to flow towards that to make larger bubbles which approach the diameter of the pipe.

- **Churn flow:** With the increased flow velocity, the flow pattern becomes unstable with the fluid travelling up and down in an oscillatory motion in the pipe with a net upward flow. This instability eventually has broken down the slug flow bubbles. This flow pattern is an intermediate regime between the slug flow and annular flow regimes. Churn flow is typically a flow regime to be avoided in two-phase transfer lines because the mass of slugs may have a destructive consequence on the piping system.
- **Annular flow:** Liquid flows on the wall of the tube as a film and the gas flows in the centre. In certain situations, there will be some concentration liquid drops entrained in the central of gas core increases which lead to large clouds of liquid and this is known as **wispy annular flow**. This flow regime is particularly stable and also is the desired flow pattern for two-phase pipe flows.

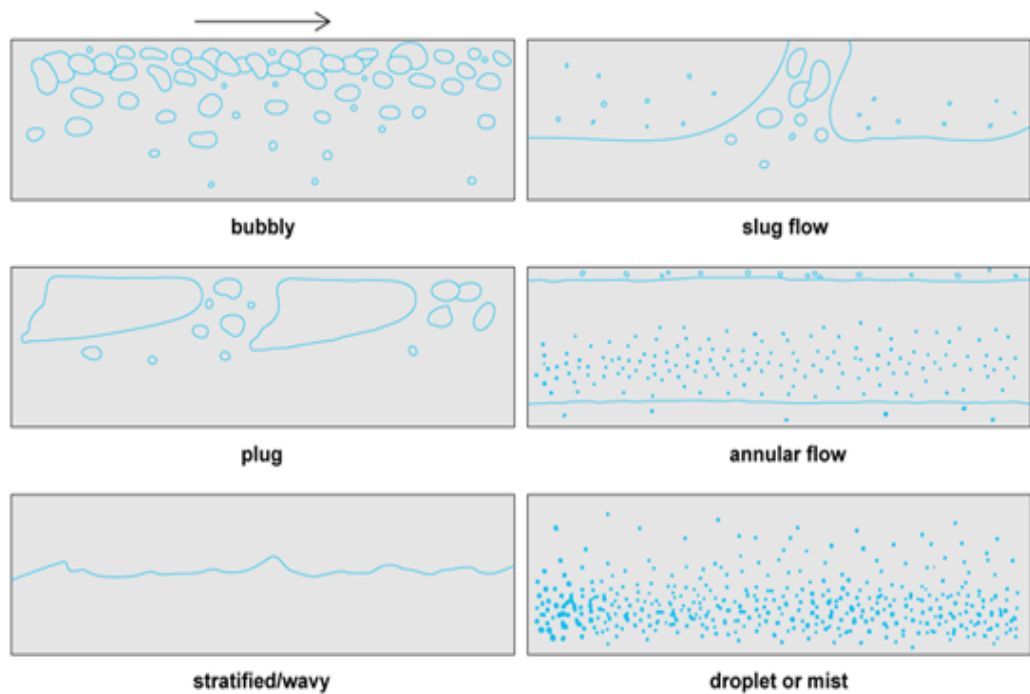


Figure 2.1 Two-phase flow patterns in vertical pipes (Wren, 2001)

2.1.2 Horizontal flow in pipes

Two-phase flow patterns in horizontal pipes are similar to those in vertical flows but the distribution of the liquid is influenced by gravity. When the gravity acts perpendicularly to the pipe axis, liquid is stratified to the bottom of the tube and the gas to the top and therefore the separation of phases occurred. Hence, Baker (2003) and Wren (2001) outlined several flow patterns for co-current flow of gas and liquid in a horizontal pipe which shown in Figure 3 and they are categorized as follows:

- **Bubbly flow:** The equivalent pattern in vertical flow. The gas bubbles are dispersed in the liquid with a high concentration of bubbles in the upper part of the pipe due to buoyancy forces. At a very high liquid velocity, mass flow rates or when the shear forces are dominant, the intensity of the turbulence is enough to disperse the bubbles uniformly in the pipe. Gravity tends to make bubbles accumulate in the upper part of the pipe.
- **Stratified flow:** Complete separation of the two phases occurs at low liquid and gas velocities. The gas goes to the top and the liquid to the bottom of the tube, separated by smooth horizontal interface. Hence, the liquid and gas are fully stratified in this regime. However, an increase of gas velocity causes waves to form on the interface of stratified flow to yield **wavy stratified flow**.
- **Intermittent flow:** Interfacial wave become larger with further increased gas velocity. This type of flow is composite of plug and slug flow regimes. These subcategories are categorized as follows:
 - **Plug flow:** This flow regime has liquid plugs that are separated by elongated gas bubbles. The large bubbles travelling along the top of the pipe whereby large waves are present on the stratified layer. Plug flow is also sometimes referred to as elongated bubble flow.
 - **Slug flow:** At increased gas velocities, the gas bubbles are larger until become similar in size to the pipe diameter. The liquid slugs separating such elongated bubbles can also be described as large amplitude waves. These waves touch the top of the tube and form a liquid slug which passes rapidly along the channel.

- **Annular flow:** As the gas velocity increased, the liquid forms a continuous annular film around the perimeter of the pipe, similar to that in vertical flow but the liquid film is thicker at the bottom than the top due to gravity.

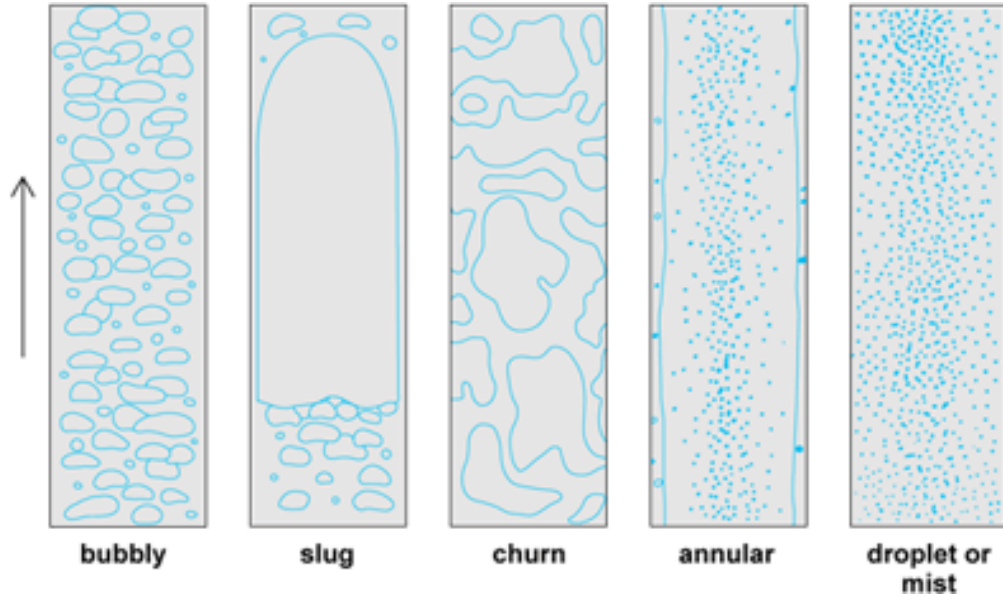


Figure 2.2 Two-phase flow patterns in horizontal flows (Wren, 2001)

2.2 Flow Pattern Identification

Baker (2003) states that there are several flow pattern identifications such as follows:

2.2.1 Visual observations and optical techniques

This is the simplest method to determine the gas-liquid flow patterns by merely observing them flowing along a transparent pipes. However, this is not feasible because of high gas and liquid flow rates. Such methods are not practiced in industrial pipelines because the existing piping systems are not transparent. Apart from that, the author also explained the optical methods. These techniques have the potential in determining the flow pattern by observing the time traces of the voltage signal.

2.2.2 Photon Attenuation Technique

This method has been widely applied and is based on the absorption of x-rays or gamma rays by liquid phase and its relationship to the void fraction. Typical probability density functions of the void functions of the void fraction variations they used to identify flow patterns are shown in Figure 2.3. Such probability density function techniques because the main tool in assessing various other measurable parameters for flow pattern determination. The rays can either come along a single beam as employed by Jones and Zuber (1975) or from an array of multiple beams across the flow path as used by Smith (1975). Apart from that, Jones and Zuber (1975) used x-ray absorption, which highlighted the usefulness of statistical analysis techniques for flow pattern determination.

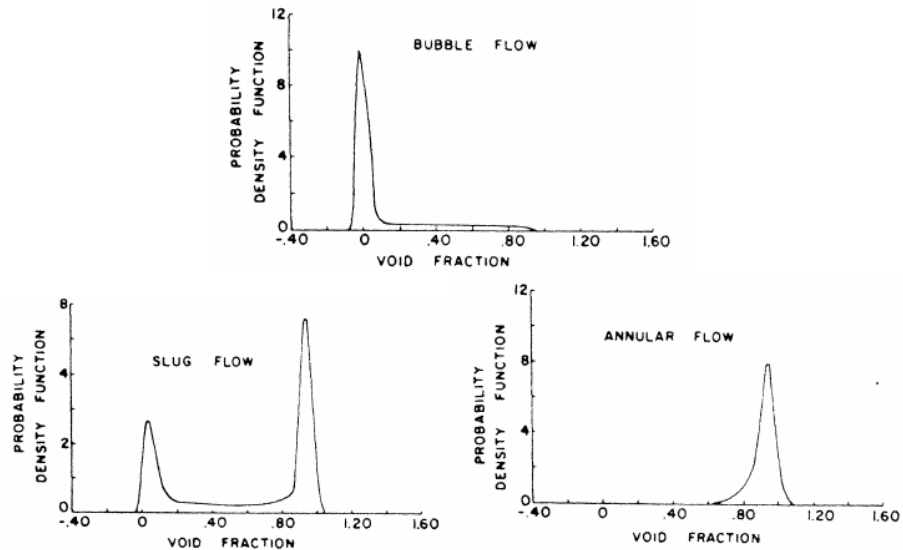


Figure 2.3 X-ray absorption probability density functions of void fractions (Jones and Zuber, 1975)

2.2.3 Pressure fluctuations

This is another method been used to identify the flow patterns. According to Baker (2003), he reported that Hubbard and Dukler (1966) developed a method to determine the flow pattern from the spectral distribution of the wall pressure fluctuations. Besides that, Weisman *et al.* (1979) developed a simple criterion for the determination of the flow pattern based on the pressure drop between two

pressure taps 0.15m apart. The criteria were primarily based on the ratio of amplitude of a “standard slug”. After this, Cai *et al.* (1996) have attempted to apply chaos theory to time traces of pressure fluctuation signals, with the aim of identifying the flow pattern transitions. The author concluded that the pressure fluctuations have the potential for flow identification even though the software and algorithms required intensive development before they could be practically used.

2.2.4 Conductance Probes

Barnea and Taitel (1985) pointed out there are two different methods used for conductance measurements which are the insertion into the flow and flush-mounted around the pipe wall. The current from the flow is measured and the generated time trace is then used to represent the distribution of the phases and the flow pattern as well. Barnea *et al.* (1980) developed an improved conductance probe method which applicable to all flow patterns and did produce satisfactory characteristic profiles for all flow patterns. The design is applicable for vertical, horizontal and slightly inclined pipes as shown in Figure 2.4.

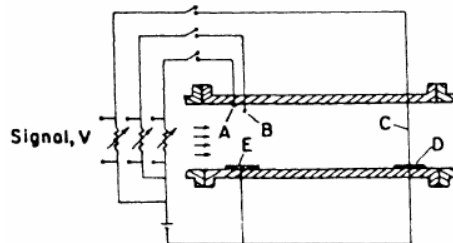


Figure 2.4 Electrode configurations for conductance method (Barnea *et al.*, 1980)

2.2.5 Tomography Imaging

Jeanmeure (2001) reported that tomography imaging is a more complex sensor design which produces imaging of the two-phase flow within the pipe. Tomographic sensors are able to produce a graphical representation of the cross-sectional flow inside the pipe. A typical layout of a process tomography system is shown in Figure 7. Initially, the sensor receives the signals and transfers them

to a data acquisition module. The signals are then further processed in computer to produce a reconstructed image representing the cross-sectional phase distribution within the pipe. This entire process can be completed in less than 0.04 seconds. The author reported that there are two types of tomography imaging which are ultrasound computerized tomography and electrical tomography.

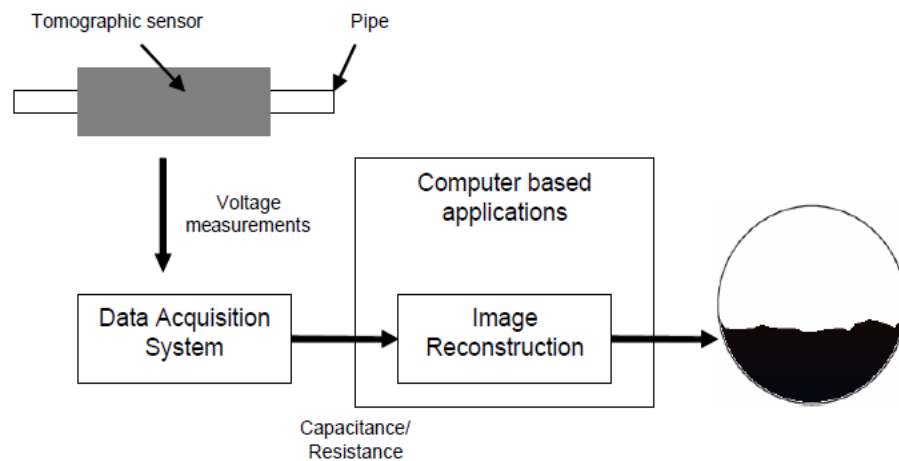


Figure 2.5 Layout of process tomography applications (Baker, 2003)

2.3 Influence of dominant forces on separation efficiency in a T-junction

According to Wren (2001), there are three dominate forces influencing the phase separation in T-junction which are the effect of gravitational acceleration, inertia and pressure drop at T-junction. Basically, the effect of gravitational acceleration acts mainly on the liquid phase. When the side arm is orientated in a downwards direction, this effect is able to draw the liquid phase down to the side arm. Correspondingly, it is able to help to reduce the fraction of liquid taken off when the side arm is vertically upwards.

Moreover, he also stated that the effect of inertia can be more significant on separation efficiency when the diameter of the side arm is smaller than the main arm and run arm of the pipe. Due to the higher axial momentum flux of the liquid tends to force the liquid to continue flowing along the pipe, passing through the smaller opening more

rapid and hence, there will be lesser time to be affected by any taken off effects for liquid phase.

Lastly, Wren concluded that pressure drop is another major contributor in affecting the flow split in T-junction. This effect can be more pronounced when the diameter of side arm is smaller than the rest of the arms which have the same diameters. He stated that the gas velocity increases significantly for the same initial gas saturation into a smaller side arm and consequently creates a larger pressure drop by Bernoulli's equation which promotes the liquid into the side arm.

2.4 Effect of variation diameter ratio on two-phase split in T-junction and mitigation of phase splitting

2.4.1 Uniform diameter of T-junction

According to Suzanne and Choi (1998), less liquid was observed to split to the side-branch resulting in higher quality as the inlet liquid volume fraction increased in a uniform diameter T-junction. However, according to Azzopardi *et al.* (2000), the degree of phase separation seems to depend on the transit time between liquid-gas mixtures and the junction. The slower flows have more time to separate both phases. Apart from that, Liu, *et al.* (2011) concluded that gas phase tend to flow into the side arm for bubbly flow is due to the pressure difference of the side arm to main arm is much larger than that for the run arm. Thus, the lower density gas will respond more easily to pressure gradient than liquid phase for the same pressure force. It is also found that the inertia difference will also eventually results in the flow split phenomenon due to large density difference. In addition, Margaris (2007) reported that the separation efficiency at uniform T-junction depends mainly on phase momentum, the existing flow pattern before the junction and also the gravity forces distribution on T-junction.

2.4.2 Reduced diameter of side arm

Baker (2003) also discussed about the effect of reduced diameter of side arm. He stated that a reduction in the side-arm diameter will have two different effects which are the associated pressure drop and the axial distance available for take-off. The division of

the phases at a T-junction but also on the two downstream pressures and the pressure drop across the junction itself. The outlet with lower pressures or greater suction, has a stronger influence on the flowing fluids and hence more significant the diversion in that direction.

Besides that, according to Wren (2001), the main difference between a reduced and a regular T-junction is the pressure redistribution around the junction. For the same inlet conditions, the reduced side-branch associates a higher pressure drop compared with the uniform T-junction. This is mainly due to the higher gas phase velocities encountered in the reduced side-arm for the same fraction of inlet gas flowing down the side arm. Wren *et al.* (2005) addresses much of the liquid film that is dragged by the gas towards the side arm may only arrive at the side wall after passing the opening of the reduced side arm. Thus, there is reduced fraction of liquid take off at side arm.

Griston and Choi (1998) also reported that the percentage of liquid split to the side-arm decreased further as the inlet vapor velocity decreased. The field tests results showed that reduced side-arm diameter further decreased the percentage of liquid split to the side-branch. The liquid have lesser tendencies to flow through the restricted cross-sectional area of the side-arm. Furthermore, Azzopardi (1999) also concluded that the effect of diameter ratio is strongest at lower gas rates and least at high gas and lower liquid flow rate conditions.

2.4.3 Mitigation of phase splitting

Suzanne and Choi (1998) mentioned about the use of SpliTigator Tee is also a device for mitigation of phase splitting. It was specifically designed to provide 70% quality to the side branch over a wide range of inlet conditions and vapor split ratios. However, the nearly proportional phase splitting was only observed at high inlet qualities (70% to 80%) and the results proved that the use of T-separator did not improve the phase splitting except for low inlet volume fraction. It is also reported that the test of adjustable flow splitting tee resulted in an easy steam quality adjustment and stable outlet conditions were achieved within a few minutes.

2.5 Effect of inclined branched arm on flow splitting behavior in T-junction

As mentioned before, gravity forces have a strong effect on the flow split especially as the orientation of the branched arm is altered. According to Baker (2003), he stated that more liquid is drawn into the branched arm when it is inclined downwards. Besides this, Penmatcha (1996) also concluded that for the higher liquid flow rate, the gravity forces acting on the liquid phase is very large that the effect of the pressure drop in the side arm is not significant until about 55% of the gas is diverted into the branched arm. However, as the liquid flow rate decreases, more liquid will be easier to divert to the branched arm due to the lower inertial forces. A few sets of experiment runs been carried out by Penmatcha (1996) and the proposed model as illustrated in Figure 2.6 is to develop a method to predict the fraction of liquid going into the branched arm and the downward orientation of the branched arm, Θ . The results shows that as the branched arm is inclined more downward, more liquid will be diverted to the branched arm until it reaches -60° downward inclination whereby almost 100% of the liquid is diverted into the branched arm resulting in a complete phase separation. As for this configuration of T-junction, he also concluded that any further lowering of the branched arm inclination over -60° would not yield any new results since the T-junction acts as a separator where all the liquid is diverted into the branched arm.

Conversely, a significant amount of the inlet gas has to be diverted up the branched arm for an upward inclination before any of the liquid is drawn off. There is only a little gas has to be diverted to draw up all of the liquid once the liquid has started to flow up the branched arm. Using the same model as shown in Figure 2.6, the results show that more diverted gas is required to start the liquid flowing into the side arm for higher upward inclination angle. Penmatcha concluded that once the branched arm is inclined at 35° , over 80% of the inlet gas has to flow into the side arm for any of the liquid to flow into that arm. At this particular inclination angle, the T-junction can act as a simple separator.

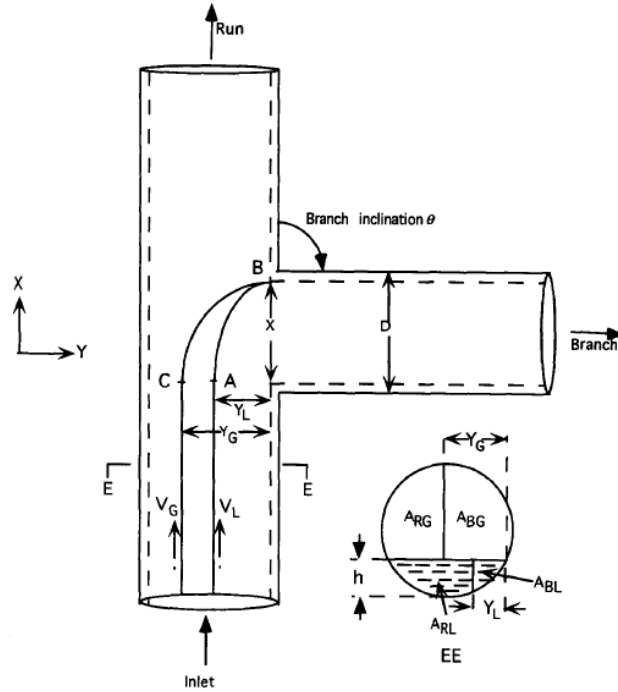


Figure 2.6 The physical model for gas and liquid splitting at T-junction (Penmatcha, 1996)

2.6 The approaches of two-phase flow split prediction

According to Liu *et al.* (2011), there are several efforts to predict the phase split situations in T-junctions. There are phenomenological-based approach, analytical model and computational fluid dynamic (CFD) simulation. The first phenomenological method considers the centrifugal force to be the dominant driving force for both the phases to flow into the side arm. Azzopardi (1999) proposed that the gas and liquid phase diverted into the side arm all came from an angle of the inlet main arm. In order to study the effect of diameter ratio on flow split, he manipulated the diameter of side arm and observed the results based on the visual inspections of the experiment. Hwang *et al.* (1988) introduced the concept of “dividing streamline” and a phenomenological model is established to predict phase flow split. According to him, the zone of influence is defined as an arc region in the main arm. The ratio of the occupied arc area to the main arm area determines the proportion of the gas phase taken off into the side arm for a fixed liquid taken off value. The “zone of influence” of gas phase is bounded by “dividing streamline” as shown in Figure 2.6. This position is calculated by presuming

that the ratio of the centrifugal radius of both gas and liquid phases approaching the junction equivalent to the dynamic pressure.

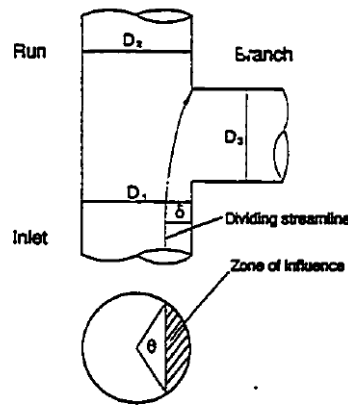


Figure 2.7 Zone of influence (Azzopardi *et al.*, 1982)

The second method to predict the flow split phenomenon which is the analytical model is illustrated by Margaris (2007). The model expresses the pressure, mass balance, momentum balance and energy balance by separate correlations in which the extensive experimental correlations are adopted.

Lastly, the third method to predict flow split is the Computational Fluid Dynamics (CFD) approach where the inertia difference of the two-phases affects the flow split, due to the density difference which leads to inertia difference. Liu *et al.* (2011) presented his flow split study using this method which considers the bubbly flow approaching the main arm. This type of flow is very common flow pattern in industrial engineering. He developed a general three-dimensional, two-fluid numerical model and presents its application to two-phase dispersed bubbly flow through a T-junction with round cross sections and the phase split phenomenon is analyzed. The experimental data of Davis and Fungtamasan (1990) was used to make comparisons for validation purpose. Besides, Issa and Olivera (1994) developed a three dimensional rectangular cross-section T-junction to study the phase split and concluded that the phases separation is due to inertia difference.

2.7 Basic theory of separation efficiency in T-junction

According to Puspitasari *et al.* (2012), separation efficiency mainly best describes the results of phase separation and the optimization of operating conditions in T-junction. Figure 3 shows the main parameters of two-phase flow in T-junction. x is the quality of gas which also known as the gas saturation and \dot{m} refers to the mass flow rate.

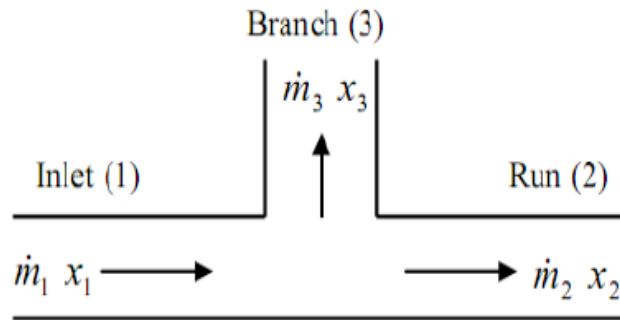


Figure 2.8 Two-phase flow parameters in the T-junction (Puspitasari *et al.*, 2012)

Hence, Puspitasari *et al.* (2012) stated the fraction of kerosene and water leaving the inlet to the side arm can be written as:

$$\text{Fraction of kerosene, } F_k = \frac{\dot{m}_{k3}}{\dot{m}_{k1}}$$

$$\text{Fraction of water, } F_w = \frac{\dot{m}_{w3}}{\dot{m}_{w1}}$$

Puspitasari *et al.* (2012) also concluded that the result of phase separation in the T-junction is presented by ratio of phase fraction taken off as show in Figure 2.8 where **k** and **w** subscript of kerosene and water phase.

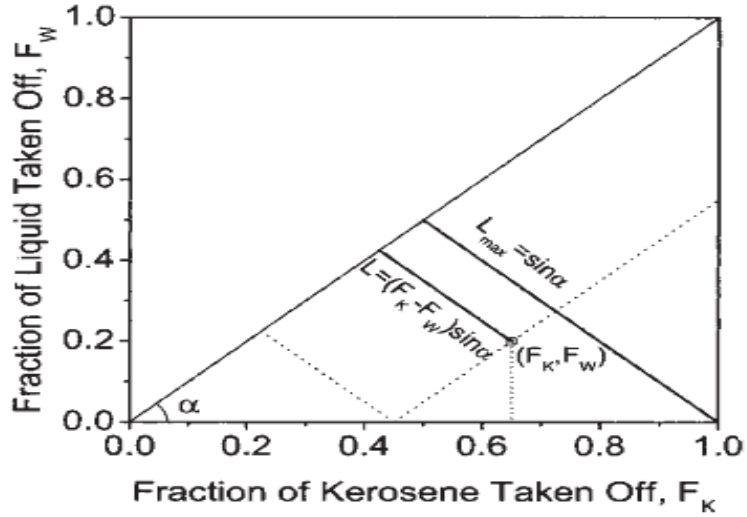


Figure 2.9 Split ratio at T-junction (Puspitasari *et al.*, 2012)

Puspitasari *et al* (2012) mentioned that the ideal separation occurs when the separation efficiency is 100% which falls at point (0, 1) or (1, 0) from Figure 2.8. On the other hand, point (1, 1) and (0, 0) indicate zero separation occurs in T-junction.

2.8 Related governing equations for gas-liquid flow in T-junction

Liu *et al.* (2011) explained his model solves full steady three-dimensional, two-fluid transport equations, where both phases are treated as interpenetrating continua distinguished by a volume factor in Eulerian frame. Turbulence is described by the standard $k-\varepsilon$ model. The equation model presented by Liu *et al.* (2011) is as follows:

Continuity equation for gas phase

$$\frac{\partial}{\partial t}(\alpha_g \rho_g) + \nabla \cdot (\alpha_g \rho_g \vec{u}_g) = 0 \quad (2.1)$$

Continuity equation for liquid phase

$$\frac{\partial}{\partial t}(\alpha_l \rho_l) + \nabla \cdot (\alpha_l \rho_l \vec{u}_l) = 0 \quad (2.2)$$

Momentum balance equations for gas phase

$$\frac{\partial}{\partial t}(\alpha_g \rho_g \vec{v}_g) + \nabla \cdot (\alpha_g \rho_g \vec{v}_g \vec{v}_g) = -\alpha_g \nabla p + \nabla \cdot \vec{\tau}_g + \alpha_g \rho_g \vec{g} + \vec{R}_{l,g} \quad (2.3)$$

Momentum balance equations for liquid phase

$$\frac{\partial}{\partial t}(\alpha_l \rho_l \vec{v}) + \nabla \cdot (\alpha_l \rho_l \vec{v} \vec{v}) = -\alpha_l \nabla p + \nabla \cdot \vec{\tau}_l + \alpha_l \rho_l \vec{g} + \vec{R}_{l,g} \quad (2.4)$$

where v is the velocity, α is the volume fraction, ρ is the density, p is the pressure, g is the gravitational acceleration, $R_{l,g}$ is the interfacial interaction force between two phases. The interfacial interaction force depends on pressure, cohesion and other effects and is subject to the conditions such that

$$R_{l,g} = -R_{g,l}, \quad R_{l,l} = 0, \quad R_{g,g} = 0.$$

The stress tensor is given as follows:

$$\tau_i = \alpha_i \mu_i \left(\nabla \mathbf{v}_i + \nabla^T \mathbf{v}_i \right) + \alpha_i \left(\lambda_i - \frac{2}{3} \mu_i \right) \text{tr}(\nabla \cdot \mathbf{v}_i) \quad i = l \text{ or } g \quad (2.5)$$

where μ and λ are the viscosity coefficients of the constituents.

2.9 Concluding Remarks

Based on my project background study and literature review, it is clearly known that configuration of T-junction is highly affects the efficiency of two-phase separation. Apart from this, there are several dominant factors that influence the separation efficiency as well such as the fluid density difference which leads to inertia difference, pressure difference, transit time between liquid-gas mixtures in junction, existing flow pattern towards the junction and inlet gas velocity. Moreover, the quality of incoming fluid at the inlet must be taken into consideration because it also contributes to the effect on flow split.

CHAPTER 3:

METHODOLOGY

3.1 Development of model simulation

The development of numerical model simulation of T-junction for two-phase separation is based on the schematic T-junction in Figure 3.1 where it consists of the main arm (1), run arm (2) and side arm (3). Fine mesh is applied to the model and then followed by simulation using the computational fluid dynamics tool (CFD) program solver (ANSYS Fluent). Parameters such as the velocity inlet for water and gas, inlet gas saturation, flow rate weighting factor for both outlets and others are taken into consideration.

This simulation applies the Eulerian multiphase model in ANSYS Fluent in modeling of two separate, yet interacting phases. In this study, we are using the continuity equations and the momentum balance equations as follows:

$$\frac{\partial}{\partial t}(\alpha_q \rho_q) + \nabla \cdot (\alpha_q \rho_q \vec{u}_q) = 0 \quad (3.1)$$

$$\frac{\partial}{\partial t}(\alpha_q \rho_q \vec{u}_q) + \nabla \cdot (\alpha_q \rho_q \vec{u}_q \vec{u}_q) = -\alpha_q \nabla p + \nabla \cdot \vec{\tau}_q + \alpha_q \rho_q \vec{g} + \sum_{p=1}^n (\vec{R}_{pq} \dot{m}_{pq} \vec{u}_{pq} - \dot{m}_{pq} \vec{u}_{qp}) + (\vec{F}_q + \vec{F}_{\text{lift}, q} + \vec{F}_{\text{vm}, q}) \quad (3.2)$$

where q and p represent any two phases, \vec{u} = velocity, α = volume fraction, ρ = density, p = pressure shared by all phases, \vec{u}_{pq} = inter-phase velocity, \vec{g} = gravitational acceleration, \vec{F}_q = external body force, $\vec{F}_{\text{lift}, q}$ = lift force, $\vec{F}_{\text{vm}, q}$ = virtual mass force, \vec{R}_{pq} = interaction force between phase and \dot{m}_{pq} = mass transfer from pth to qth phase.

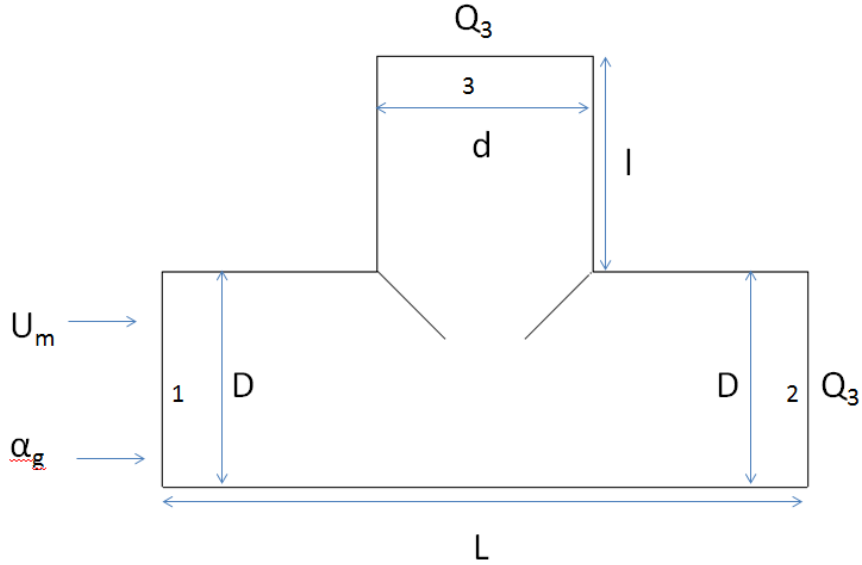


Figure 3.1 Schematic T-junction with applied inlet and outlets boundary conditions

Table 3.1 illustrates the input parameters for validations from Davis *et al.* (1990) experiment data. The lowest and highest limit range for parametric studies have been set and listed in Table 3.1 too in order to have clearer view on how the parameters above affect the phase separation.

Table 3.1 Input parameters for validations and parametric studies

Input Parameters	Validations	Present Study
Main and run arm diameter, D_1 & D_2 (mm)	50	200
Side arm diameter, d_3 (mm)	50	100, 150, 200
Total length of horizontal arm, L (mm)	1050	4200
Total length of vertical arm, l_3 (mm)	500	2000
Density of liquid phase, ρ_l (kg/m^3)	998.2 (Water)	998.2 (Water)
Density of gas phase, ρ_g (kg/m^3)	1.225 (Air)	0.6 to 0.75 0.6679 (Methane gas)
Initial gas saturation, α_g	0.47, 0.52, 0.56, 0.63	0.7 to 0.96
Inlet mixture velocity, U_m (m/s)	2.92, 6.21, 5.57, 6.62	8 to 15
Inclination angle of gravity	0°	0° to 45° (clockwise)
Overall mass split ratio, Q	0.2, 0.4, 0.6, 0.8	0.3 to 0.9
Operating pressure, P (kPa)	101.325	101.325
Averaged bubble diameter (m)	0.002	0.004

3.2 Mesh dependency check analysis

This analysis is used to study the mesh dependent convergence behavior. In order to study the convergence behavior, several runs of simulation had been performed with varying total number of tetrahedral cells. The pressure distribution in the T-junction is the criteria selected to check on the convergence behavior. Figure 3.2 shown is the computational mesh of T-junction while Figure 3.3 illustrates the convergence behavior of different mesh density based on the pressure obtained at a particular position at the T-junction. For the coarser meshes or lower mesh density, the pressure distribution at an increase initially. In other words, the error on the coarser mesh is high and it is mainly influenced by the mesh density. The curve converges as the mesh is refined and it provides much better resolution compared to a coarser mesh. The present approach resulted in approximately three hours per simulation time.

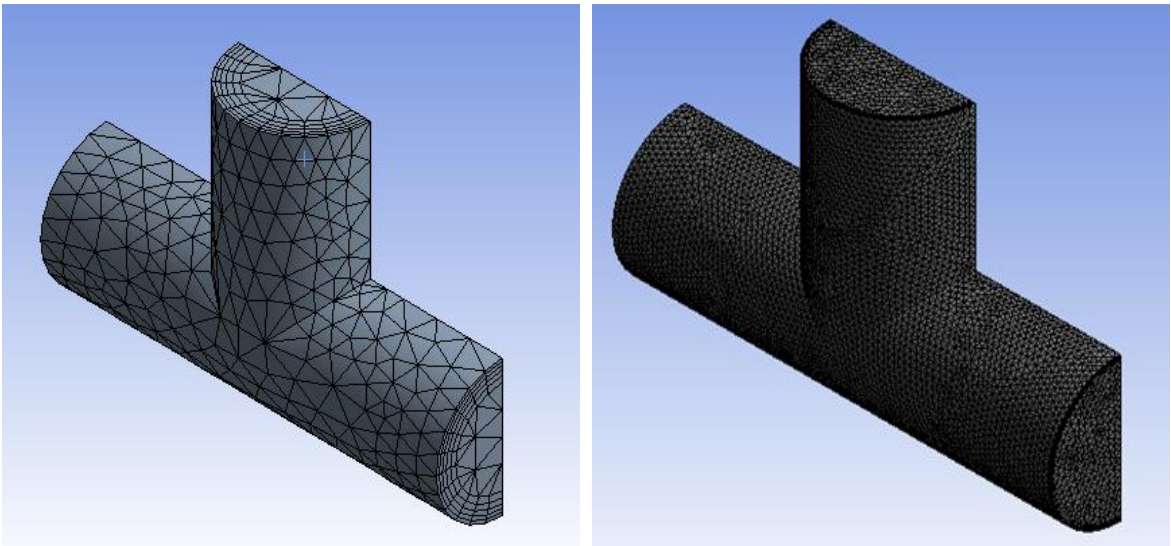


Figure 3.2 Computational mesh refinement of T-junction

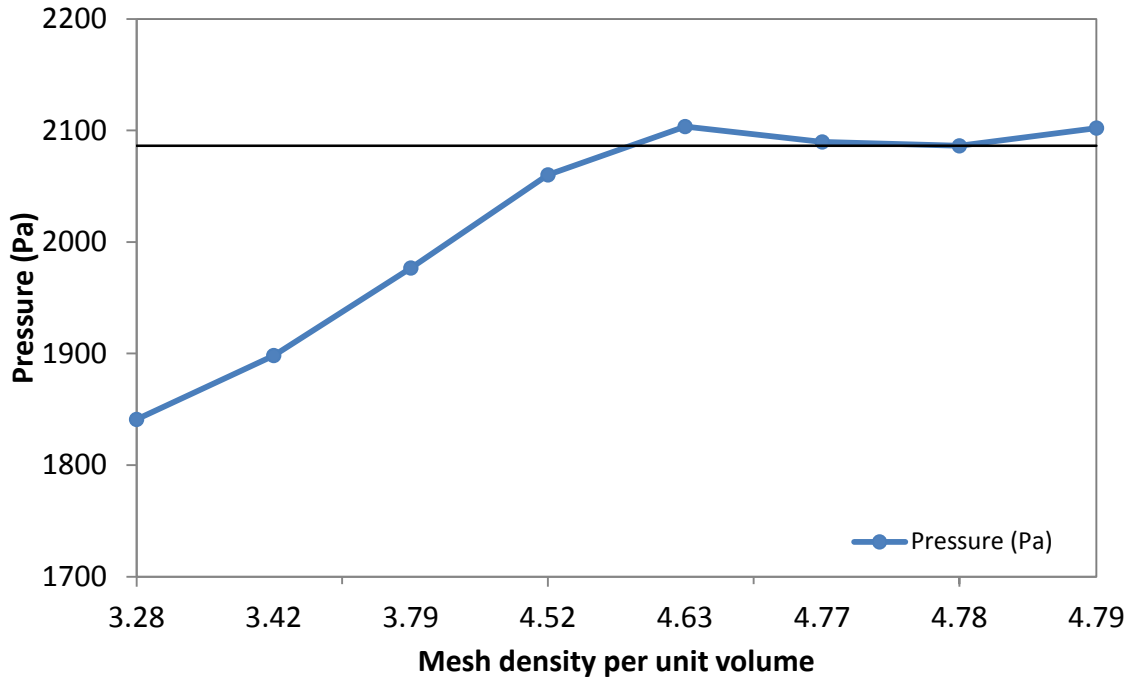


Figure 3.3 Pressure convergence versus mesh density

All the figures below illustrate the contours of the fluid phases in T-junction. Basically, the comparison are made between the coarsest mesh and the finest mesh which have total number of 4272 tetrahedral cells and total number of 253919 tetrahedral cells respectively. It is shown that the contours differ from the coarsest and the finest meshes. These depict that the contours are more precise and accurate as the mesh is refined till it reaches convergence as shown in Figure 3.3 where there is no variation of the contours.

3.2.1 Comparison of pressure contours by applying different mesh densities

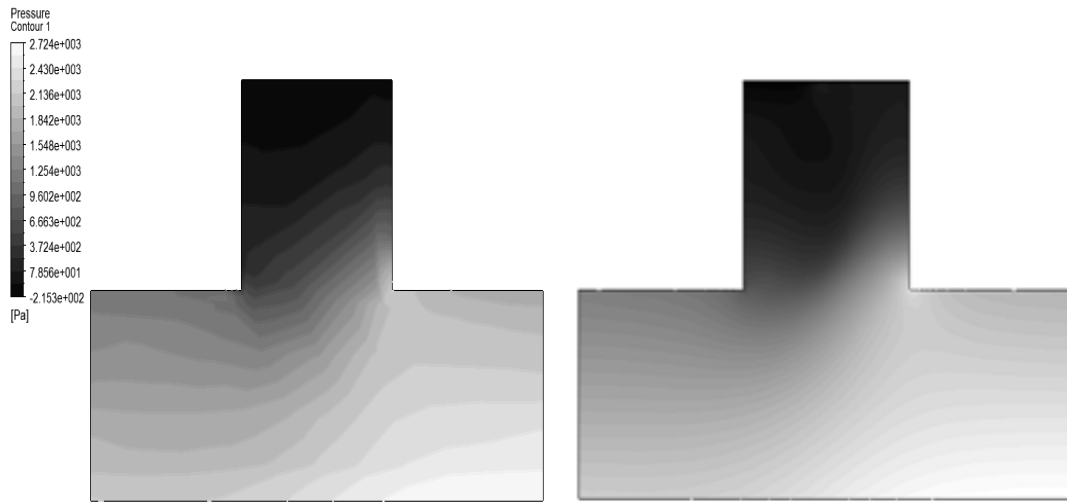


Figure 3.4 Pressure contour of mixture phase with total number of 4272 tetrahedral cells and 253919 tetrahedral cells.

3.2.2 Comparison of water velocity contours by applying different mesh densities.

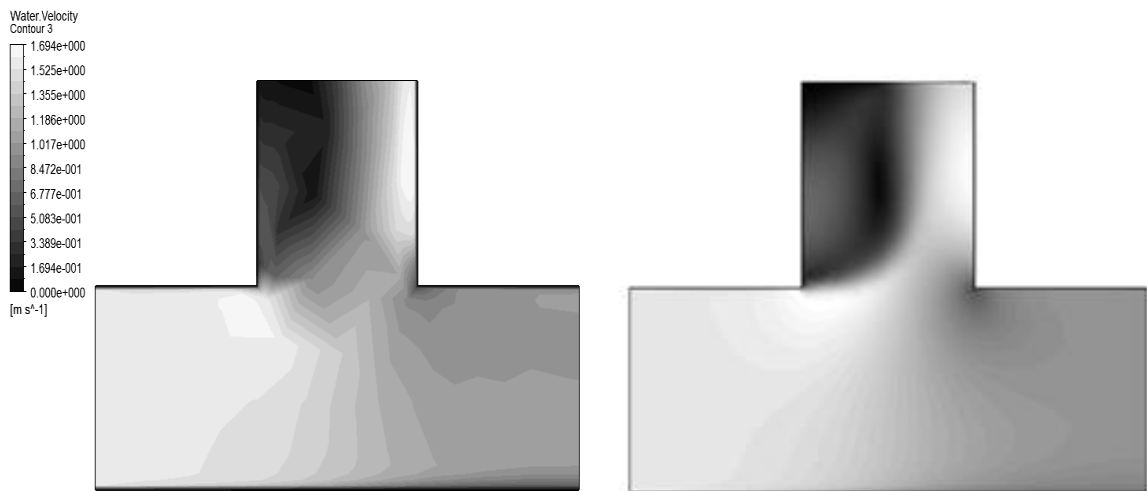


Figure 3.5 Velocity contour of water phase with total number of 4272 tetrahedral cells and 253919 tetrahedral cells.

3.2.3 Comparison of the streamlines turbulence kinetic energy contours

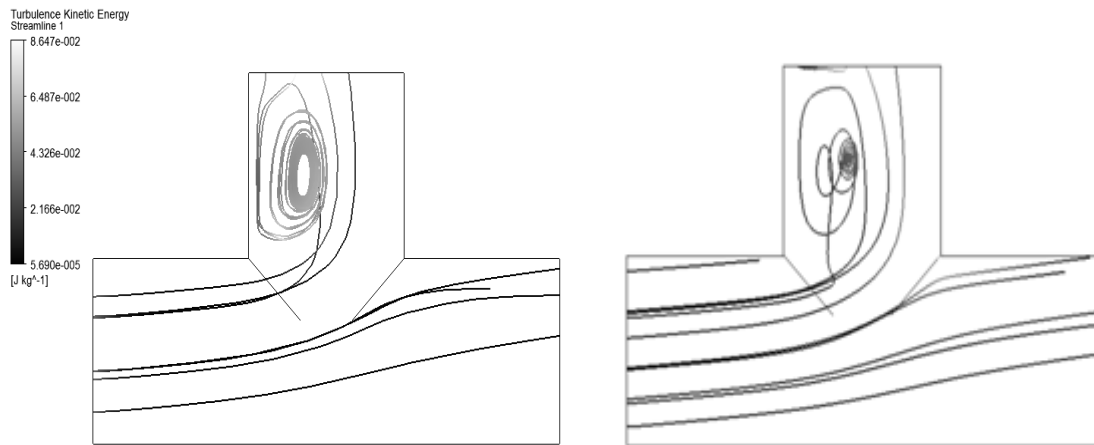


Figure 3.6 Streamlines of air velocity with total number of 4272 tetrahedral cells and 253919 tetrahedral cells.

Figure 3.7 below summarizes the process required in this study which includes the considerations of T-junction modeling, the model development, mesh dependency analysis, validations of simulation data with experimental data and lastly will be the parametric studies and results analysis via computational fluid dynamics tool.

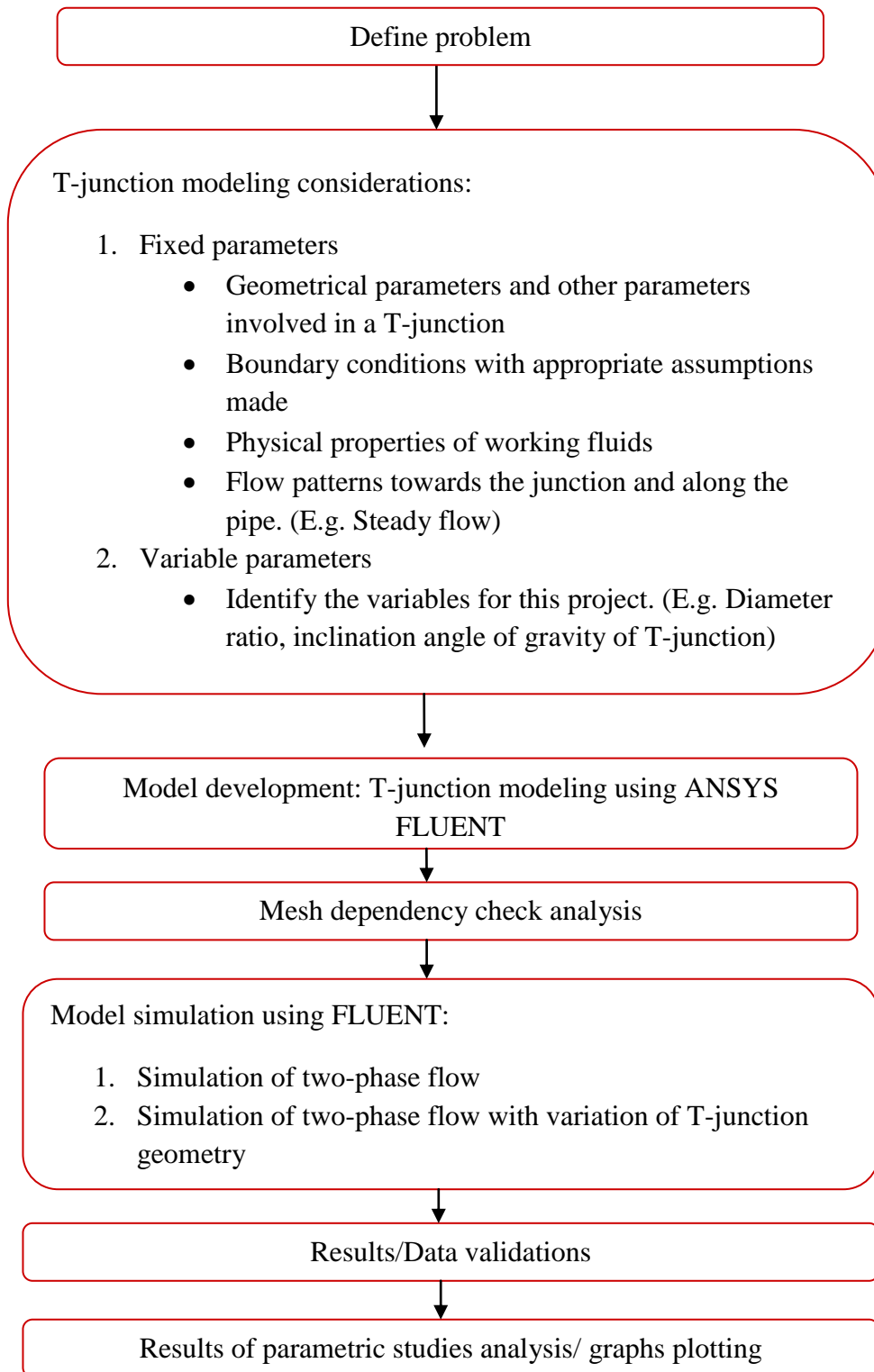


Figure 3.7 Project Process Flow Chart

3.3 Project Activities

Figure 3.8 shows the critical phases of the whole study. The project is divided into five phases which are the background study and literature review, T-junction modeling, mesh dependency analysis, model simulation, data validations and lastly parametric results analysis and graphs plotting.

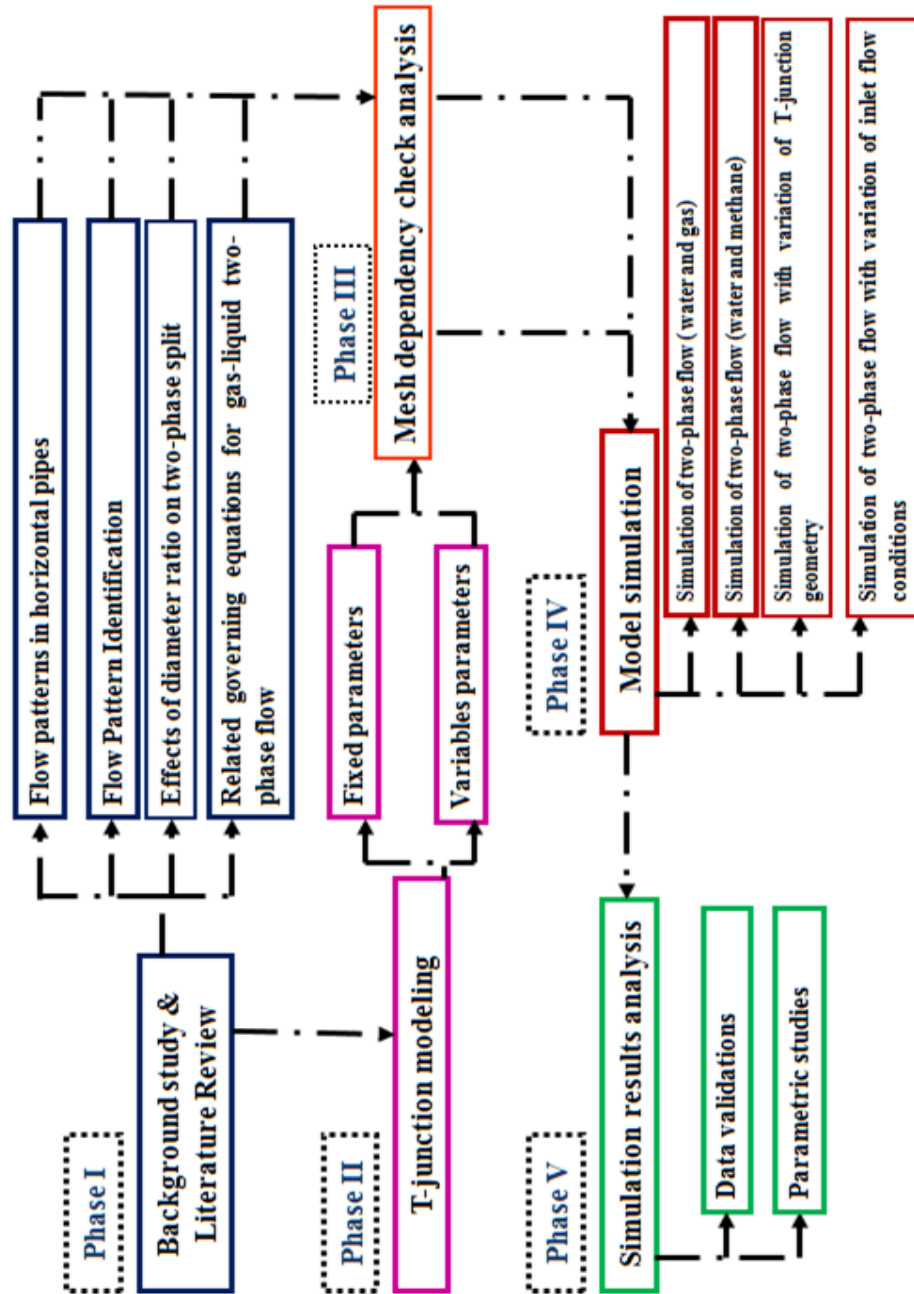


Figure 3.8 Five Phases of Project Flow Activities

3.5 Tools required

FLUENT software is commonly employed for modeling fluid flow and heat transfer in complex geometries. It is ideally suited for both incompressible and compressible fluid-flow simulations. This software is also able to provide complete mesh flexibility including the ability to solve flow problems. This project requires FLUENT software to develop the T-junction model and simulate two-phase flow splitting in T-junction.

CHAPTER 4:

RESULTS AND DISCUSSIONS

4.1 Verification of the Simulation Model with Experiment data

Davis *et al.* (1990) did an experiment to study the flow split behavior in a T-junction which provide the experiment data comparing the flow split efficiency in terms of the gas taken off value and the liquid taken off value. In this experiment set-up, a mixture of water and air bubbly flow was introduced into a T-junction with a 50mm inner tube wall diameter for all arms. The main arm was arranged vertically and the side arm was made horizontal.

A uniform velocity profile is imposed for both water and air phases at the inlet boundary, which all data samples are selected from Davis's experiments. α_g refers to the volume of gas fraction while U_m refers to the averaged inlet mixture velocity which is calculated according to:

$$U_m = \frac{\alpha_l \rho_l u_l + \alpha_g \rho_g u_g}{\alpha_l \rho_l + \alpha_g \rho_g} \quad (4.1)$$

where ρ_l and ρ_g refer to the density of liquid and gas. The detailed values of input parameters are provided in Methodology chapter, Table 3.1.

In this study, the measured overall flow split, Q_3/Q_1 is specified and this leaves the individual phase flow split to be predicted as an outcome. Lastly, no slip type is applied to the boundary condition for the tube wall. The flow parameters of four inlet flow conditions were investigated and analyzed where each flow conditions consists of four groups of overall mass split ratio which are 0.2, 0.4, 0.6 and 0.8.

The data collected from the Davis et al.'s experiment is used to compare with the data collected from the simulation model on the similar case. Figure 4.1 shows the T-junction built with 500mm for all arms with 50mm of diameter.

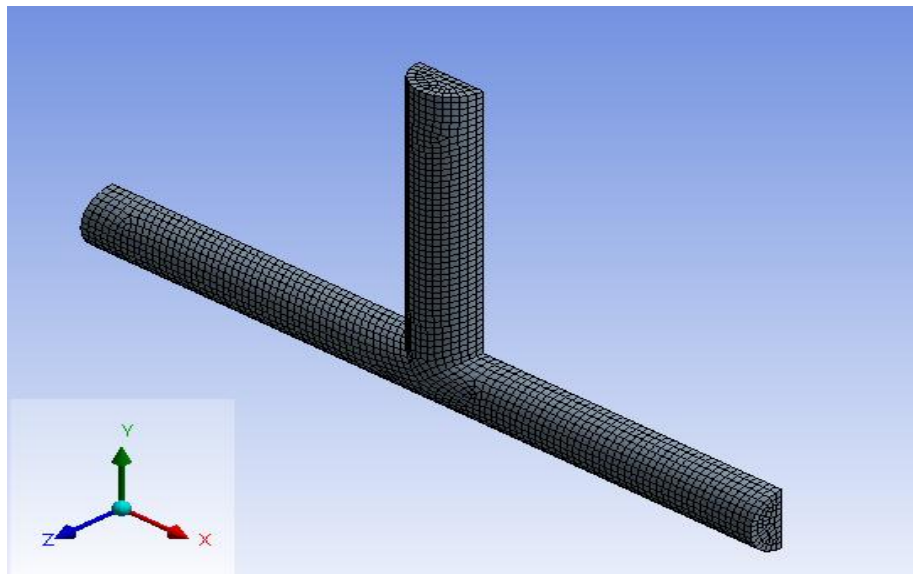


Figure 4.1 Computational grid of T-junction

The results collected from both sources are almost identical. Figure 4.2 shows the comparison of data obtained from the experiment and the simulation model for vertical side arm and horizontal main arm with averaged bubble diameter of 2mm.

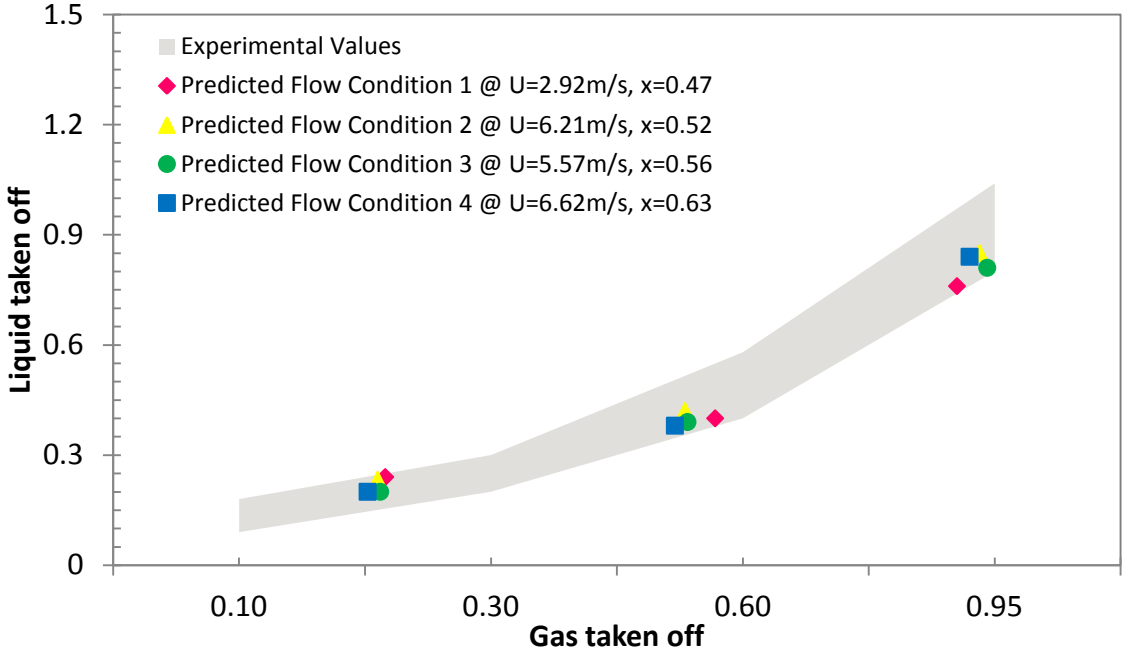


Figure 4.2 Simulated flow split curves compared with experimental results

4.2 Parametric studies on two-phase separation efficiency in T-junction

By using the simulation model that has been developed, six factors are examined which are predicted to be affecting the two-phase separation efficiency through several parametric studies for T-junction. Those variables are the diameter ratio of the main arm to the side arm, the initial gas saturation, gas densities, overall mass split ratio, averaged inlet mixture velocity of the fluids and the inclination angle of gravity. Detailed parameters of simulation model are summarized in Table 3.1 under Methodology chapter. With the listed parameters range, the resulting fraction of gas taken off is clearly shown as figures below according to the variation of input parameters.

4.2.1 Effect of Diameter Ratio on Fraction of Gas Taken Off

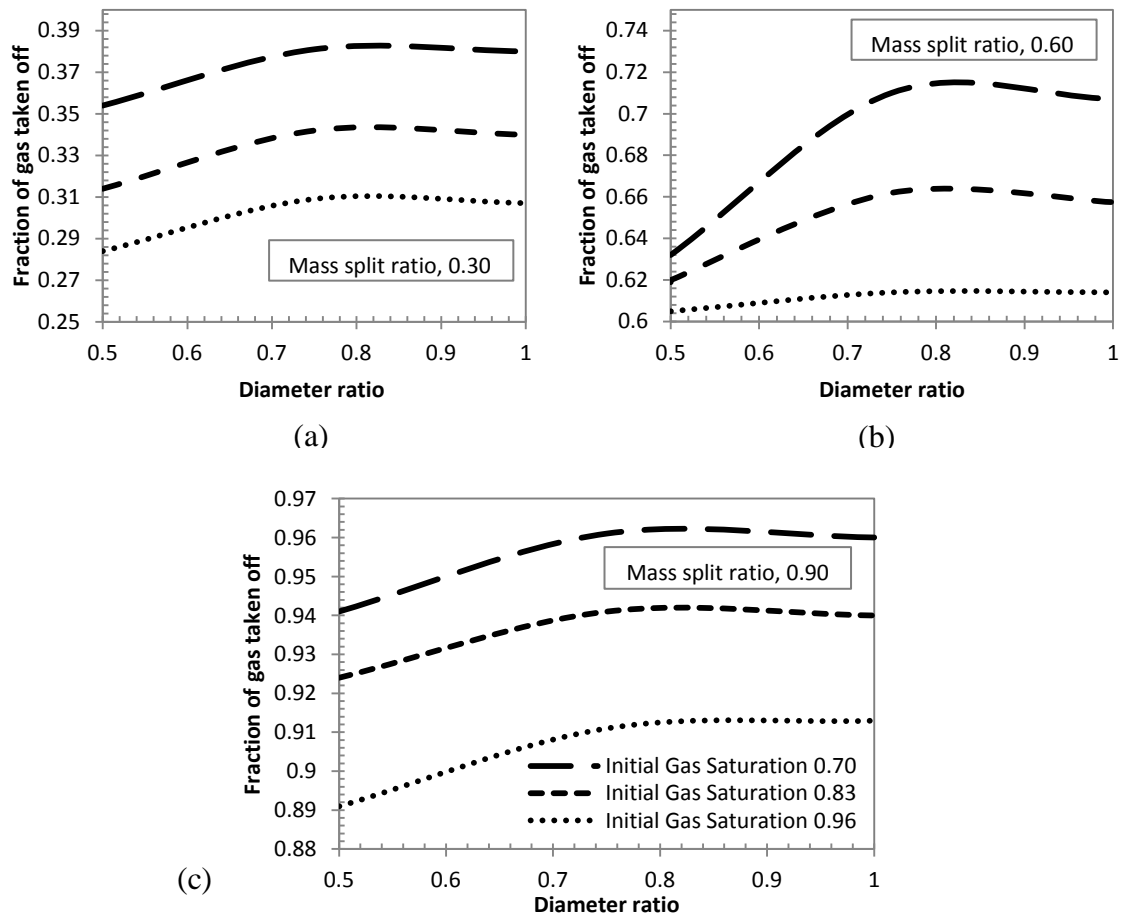


Figure 4.3 Effect of Diameter ratio on Fraction of gas taken off with initial velocity of 15m/s and Methane density of 0.6679kg/m^3

Based on Figure 4.3, the gradient of each section of the line refers to the fraction of gas taken off per unit change of diameter ratio for mass split ratio, M of 0.3, 0.6 and 0.9 with initial gas saturation, S_g of 0.70, 0.83 and 0.96, are summarized as Table 4.1.

Table 4.1 Fraction of gas taken off per unit change of diameter ratio for mass split ratio, M of 0.3, 0.6 and 0.9.

Initial Gas Saturation, S_g	Diameter Ratio, D	Gradient		
		$M = 0.3$	$M = 0.6$	$M = 0.9$
0.70	0.50 to 0.75	0.108	0.312	0.080
	0.75 to 1.00	-0.004	-0.012	-0.004
0.83	0.50 to 0.75	0.112	0.172	0.068
	0.75 to 1.00	-0.008	-0.018	-0.004
0.96	0.50 to 0.75	0.100	0.036	0.080
	0.75 to 1.00	-0.008	0.000	0.008

Based on the Table 4.1, it shows that the fraction of gas taken off increases as the diameter ratio increases from 0.50 to 0.75 and results in an increase of fraction of gas taken off per unit change of diameter. However, the effect of diameter ratio on fraction of gas taken off is diminishing as the diameter ratio increases from 0.75 to 1.00 which results in a negative gradient. As for mass split ratio of 0.6, it is shown that the fraction of gas taken off increases drastically from diameter ratio of 0.50 to 0.75 for initial gas saturation of 0.70. This results in the greatest fraction of gas taken off per unit change of diameter ratio among Figure 4.3 (a), (b) and (c). In other words, the change of gradient of $M = 0.30$ and 0.60 implies the fraction of gas taken off per unit of diameter ratio per mass split ratio radically especially when the initial gas saturation of 0.70. The fraction of gas taken off increases from diameter ratio of 0.50 to 0.75 too for mass split ratio of 0.90 which results in an increase of fraction of gas taken off per unit change of diameter ratio. In brief, Figure 4.3 depicts the optimum performance of a T-junction takes place when the diameter ratio of side arm to main arm is reduced to about 0.75 where maximum fraction of methane gas is taken off. This is where it reaches the inflection point where the fraction of gas taken off will no longer increase further.

4.2.2 *Effect of Initial Gas Saturation on Fraction of Gas Taken Off*

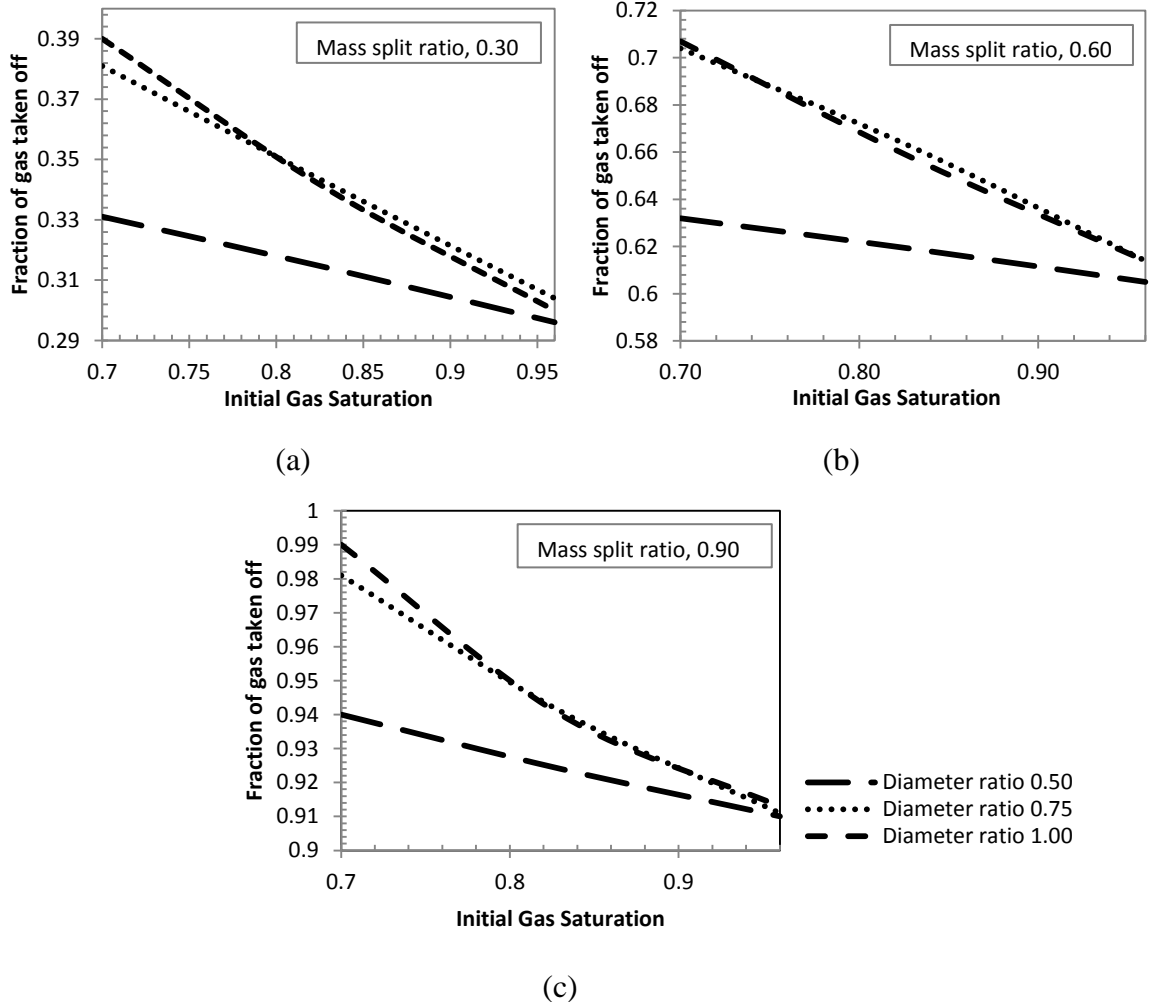


Figure 4.4 Effect of Initial gas saturation on Fraction of gas taken off with initial mixture velocity of 15m/s and Methane density of 0.6679kg/m³

Based on Figure 4.4, the gradient of each section of the line which refers to the fraction of gas taken off per unit change of gas saturation with variation of diameter ratio is summarized as Table 4.2.

Table 4.2 Fraction of gas taken off per unit change of initial gas saturation for mass split ratio, M of 0.3, 0.6 and 0.9

Diameter Ratio, D	Initial Gas Saturation, S_g	Gradient		
		M = 0.3	M = 0.6	M = 0.9
0.50	0.70 to 0.83	-0.134	-0.100	-0.123
	0.83 to 0.96	-0.138	-0.108	-0.108
0.75	0.70 to 0.83	-0.300	-0.323	-0.308
	0.83 to 0.96	-0.292	-0.369	-0.231
1.00	0.70 to 0.83	-0.385	-0.380	-0.385
	0.83 to 0.96	-0.308	-0.335	-0.208

Based on the Table 4.2, it shows that the fraction of gas taken off decreases as the initial gas saturation increases from 0.70 to 0.96 and results in a great decrease of fraction of gas taken off per unit change of gas saturation. From Figure 4.4 (a), (b) and (c), it is clearly illustrated the fraction of gas taken off is significantly less for diameter ratio of 0.50 compared to diameter ratio of 0.75 and 1.00. Basically, Figure 4.4 (a) and (b) show the effect of initial gas saturation on fraction of gas taken off are the same as the gradient for M = 0.30 and 0.60 does not have much difference. However, from Figure 4.4 (c), there is a minor arch which indicates the gas saturation does more affect on the fraction of gas taken off when M = 0.90 and it is proven in Table 4.2 that the gradient for initial gas saturation from 0.70 to 0.96 do have great differences compared to M = 0.30 and 0.60. In short, initial gas saturation does affect the fraction of gas taken off only when the overall mass split ratio is 0.90 whereby the diameter ratio is 0.50 and 0.75.

4.2.3 Effect of Inclination Angle of Gravity on Fraction of Gas Taken Off

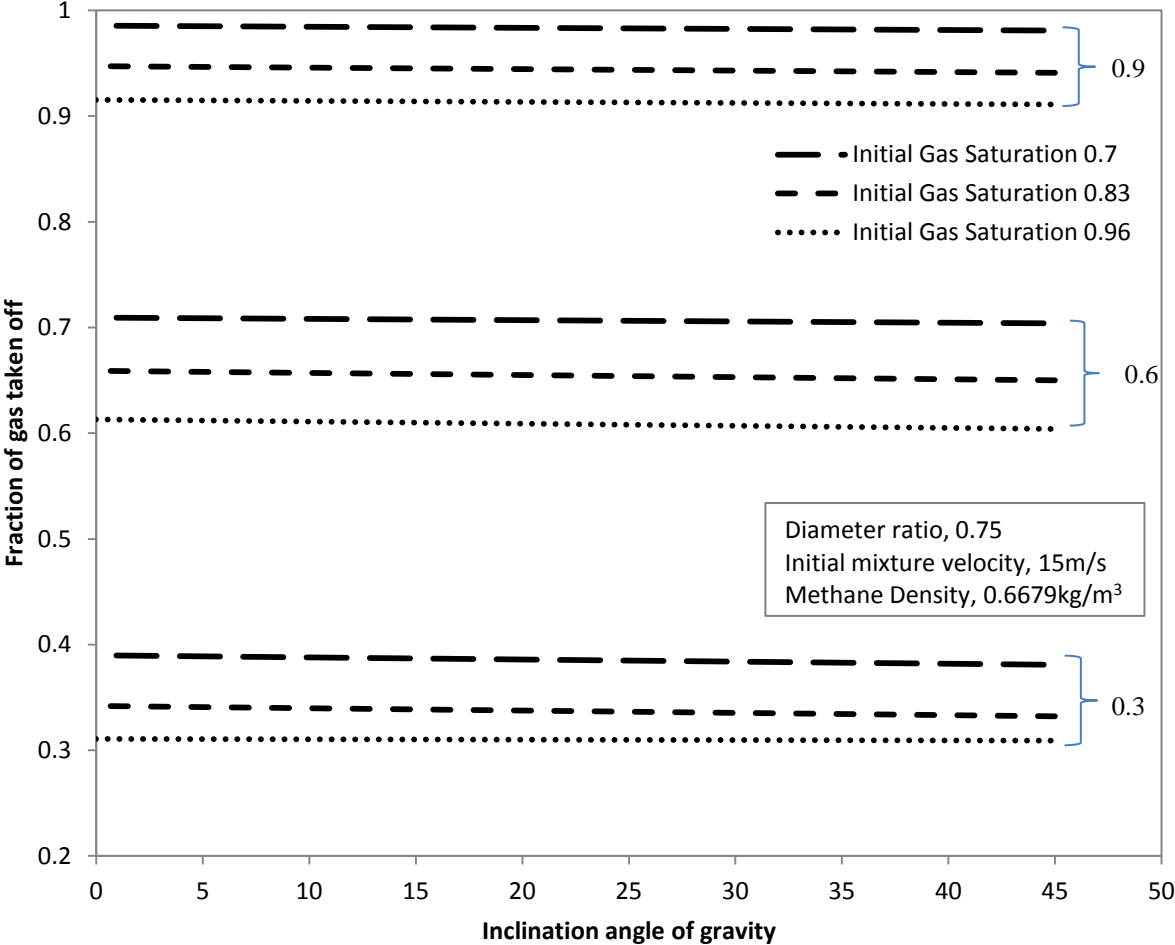


Figure 4.5 Effect of Inclination angle of gravity on Fraction of gas taken off with overall mass split ratio of 0.30, 0.60 and 0.90

The effect of per unit change of inclination angle of gravity on the fraction of gas taken for initial gas saturation of 0.70, 0.83 and 0.96 is summarized as Table 4.3.

Table 4.3 Fraction of gas taken off per unit change of inclination angle of gravity for mass split ratio, M of 0.3, 0.6 and 0.9

Initial Gas Saturation, S_g	Inclination angle of gravity, Θ	Gradient		
		M = 0.3	M = 0.6	M = 0.9
0.70	0 to 45	-0.00022	-0.00013	-0.00011
0.83	0 to 45	-0.00024	-0.00022	-0.00015
0.96	0 to 45	-0.000044	-0.00022	-0.00011

Based on Figure 4.5, it shows that the effect of inclination angle of gravity on fraction of gas taken off is very minor and this is also proven in Table 4.3 where the negative gradient for all conditions decreases insignificantly. However, among the three cases of overall mass split ratio, the effect of inclination angle of gravity is slightly greater for M = 0.30 compared with the others whereas the impact is the least when M = 0.90. Nevertheless, it is proven that this parameter does a very small impact on fraction of gas taken of per unit of inclination angle of gravity.

4.2.4 Effect of Gas Density on Fraction of Gas Taken Off

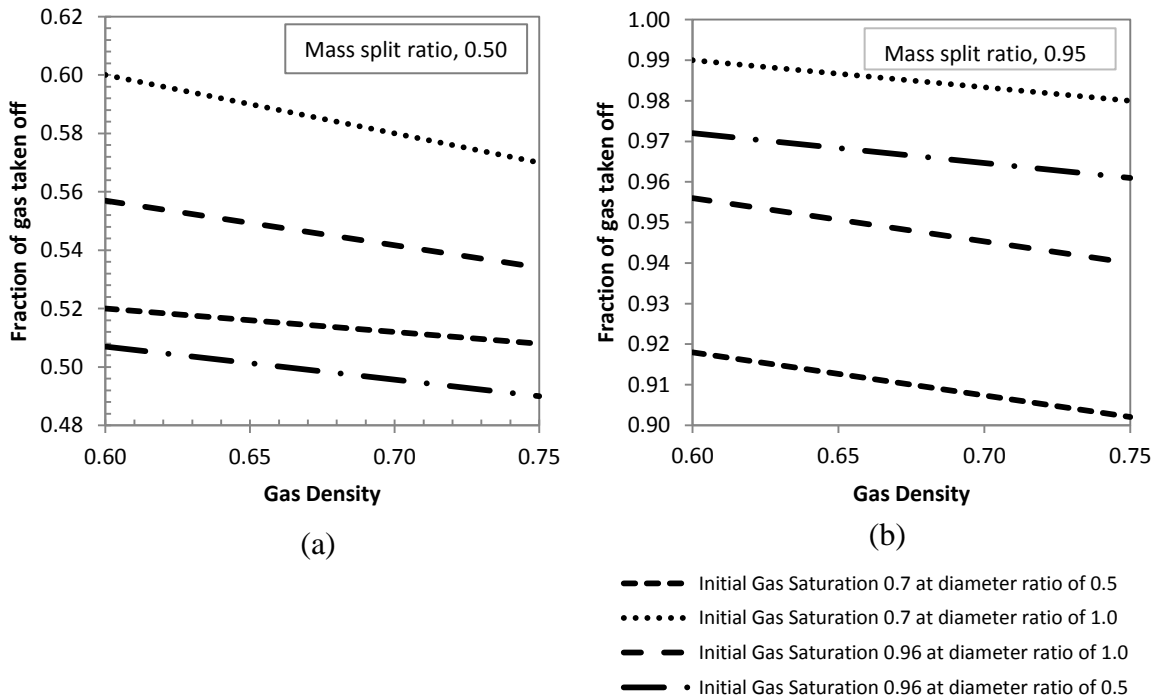


Figure 4.6 Effect of Gas density on Fraction of gas taken off with overall mass split ratio of 0.50 and 0.95 with an inlet mixture velocity of 12m/s

The inclination of straight lines from Figure 4.6 refers to the fraction of gas taken off per unit change of gas density is described as Table 4.4 for both mass split ratio, M of 0.50 and 0.95.

Table 4.4 Fraction of gas taken off per unit change of gas density for mass split ratio, M of 0.50 and 0.95

Initial Gas Saturation, S_g	Diameter Ratio, D	Gas Density, ρ_g	Gradient	
			M = 0.5	M = 0.95
0.70	0.50	0.60 to 0.75	-0.153	-0.107
	1.00	0.60 to 0.75	-0.200	-0.067
0.96	0.50	0.60 to 0.75	-0.113	-0.107
	1.00	0.60 to 0.75	-0.080	-0.073

Figure 4.6 (a) and (b) illustrates the effect of gas density is inversely proportional to the fraction of gas taken off. From Table 4.4, it summarizes that gas density has a greater effect when the diameter ratio increases from 0.50 to 1.00 when the initial gas saturation is 0.70 for both $M = 0.50$ and 0.95 . On the other hand, the gradient decreases from diameter ratio of 0.50 to 1.00 when the initial gas saturation is 0.96. This proves that the effect of gas density does affect the phase separation efficiency when the initial gas saturation is low. On top of that, the table also implies the fraction of gas taken off per unit change of gas density per mass split ratio decreases for both diameter ratio and initial gas saturation.

4.2.5 Effect of Overall Mass Split Ratio on Fraction of Gas Taken Off

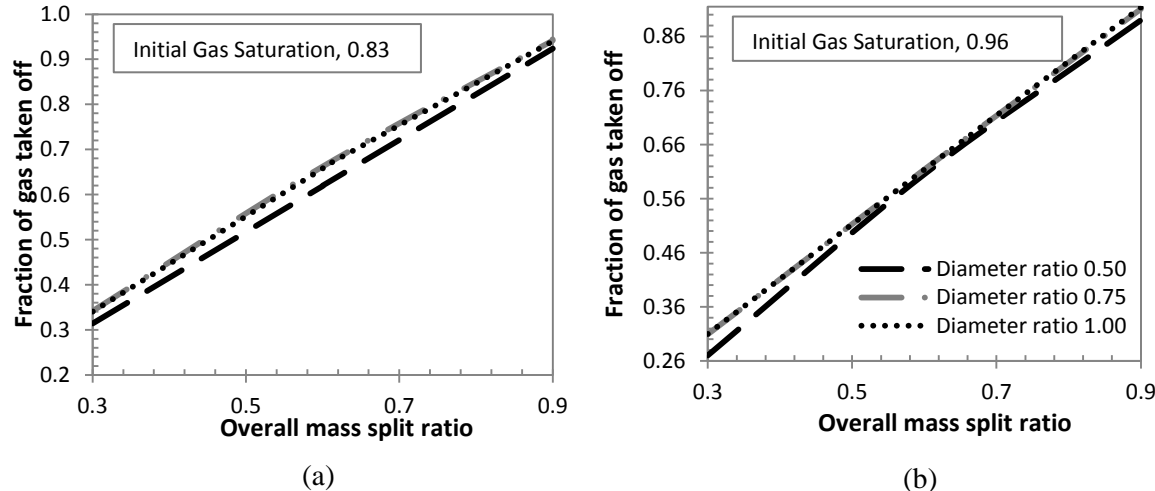


Figure 4.7 Effect of Overall mass split ratio on Fraction of gas taken off with initial gas saturation of 0.83 and 0.96 with inlet mixture velocity of 15m/s and methane density of 0.6679kg/m^3

Table 4.5 below describes the fraction of gas taken off per unit change of overall mass split ratio for both initial gas saturation, S_g of 0.83 and 0.96.

Table 4.5 Fraction of gas taken off per unit change of overall mass split ratio for initial gas saturation, S_g of 0.83 and 0.96

Diameter Ratio, D	Overall Mass Split Ratio, M	Gradient	
		$S_g = 0.83$	$S_g = 0.96$
0.50	0.30 to 0.90	1.02	1.03
0.75	0.30 to 0.90	1.00	1.00
1.00	0.30 to 0.90	1.00	1.01

Figure 4.7 (a) and (b) illustrates the fraction of gas taken off is linearly proportional to the overall mass split ratio. From Figure 4.7 (a), it shows that the fraction of gas taken off is 0.30 when the overall mass split ratio is 0.30 when the initial gas saturation is 0.83 for diameter ratio of 0.5. Conversely, Figure 4.7 (b) shows there is a slight decrease on fraction of gas taken off for the same overall mass split ratio scale. This proves the effect of initial gas saturation on phase separation as mentioned previously at section 4.2.2, whereby the fraction of gas taken off decreases as the initial gas saturation increases. Table 4.4 implies there is a slight increase of fraction of gas taken off per unit change of overall mass split ratio per unit change of mass split ratio for diameter ratio 0.50 and 1.00 whereas for diameter ratio of 1.00, the gradient remains the same which proves that the overall mass split ratio does no further effect on fraction of gas taken off as the initial gas saturation increases.

4.3 Concluding Remarks

Based on the parametric findings, overall mass split ratio plays the most important role on phase separation. This parameter refers to the split ratio of mixture phase for both side and run arm outlets, leaving the individual phase at each outlet to be predicted. It is also clearly proven that the overall mass split ratio dominates the fraction of gas taken off. On the other hand, inclination angle of gravity does not play an important role on phase separation in T-junction. This is mainly because of the orientation of T-junction in present study is focusing on the horizontal main arm and vertical side arm whereby the liquid is intended to be remained along the main and run arms. However, further investigation of this effect with variation of side arm inclination and T-junction orientation is required to have a clearer picture on effect of inclination angle of gravity on flow splitting behavior in T-junction.

Since the phenomenon of phase maldistribution is utilized to separate the phases in different proportions among the outlet arms, hence the working fluids' density differences does affect the separation performance in T-junction. Theoretically, the lesser dense fluid will tend to divert to the side arm while the denser fluid will tend to remain at the main and run arms. From the findings, it is proven that the larger the density differences of working fluids, more gas will tend to divert to the side arm and results in greater fraction of gas taken off. Hence, this depicts that the theoretical study on phase splitting phenomenon is verified.

When dealing with a large number of parameters in solving an engineering problem, it is better to determine the more significant parameters of the outcome. Based on the parametric studies above, Figure 4.8 summarizes the weighting factors in percentage to the applied equations from lowest to highest upon the fraction of gas taken off. It illustrates that overall mass split ratio does the most impact on the phase separation, and then followed by the initial gas saturation and diameter ratio. Conversely, both averaged inlet mixture velocity and inclination angle of gravity have the least impact compared to the rest of the parameters. This figure also implies the proportionality in terms of mathematical relation and it shows that the diameter ratio, gas density difference and the overall mass split ratio are the directly proportional to the

fraction of gas taken off while the initial gas saturation, inlet mixture velocity and the inclination angle of gravity is inversely proportional to the fraction of gas taken off in T-junction.

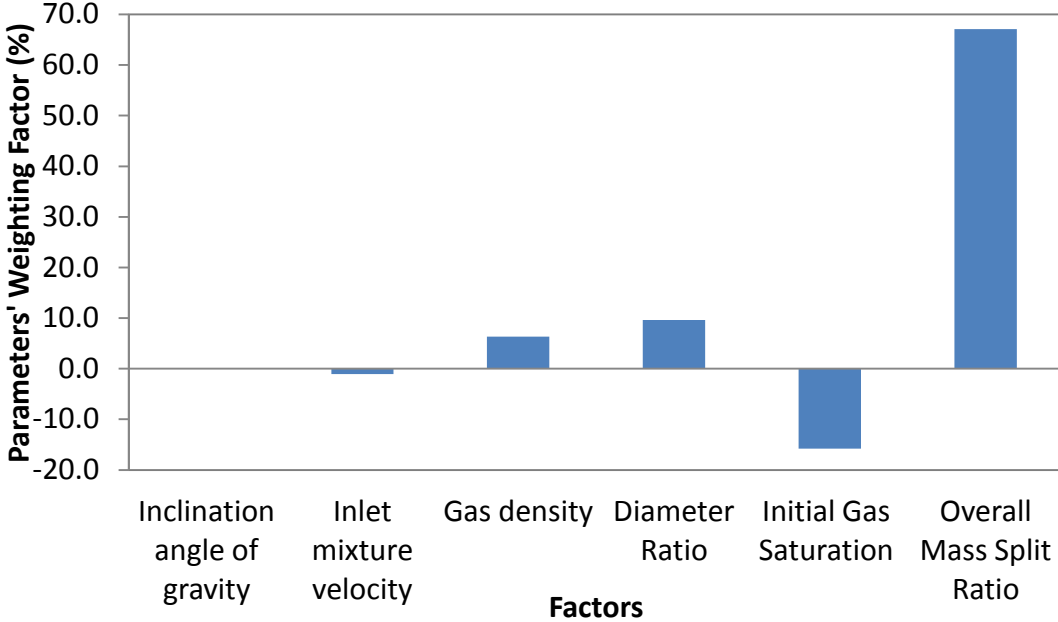


Figure 4.8 Parameters' weighting factor on two-phase separation in T-junction

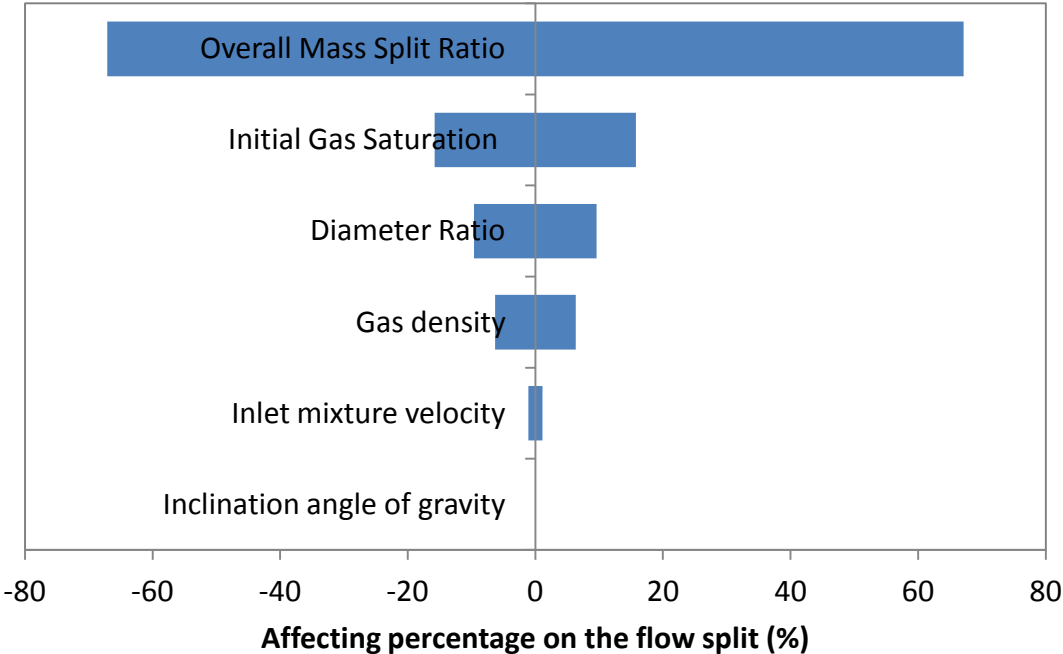


Figure 4.9 Parameters' sensitivity to fraction of gas taken off

In order to look at the parameters' sensitivity, tornado chart is constructed as shown in Figure 4.9. This chart clearly illustrates the sensitivity of parameters to the solution. It reveals that the most sensitive parameters are the overall mass split ratio, initial gas saturation and diameter ratio where all of these factors have the affecting percentage of 10% out of the six parameters. The least sensitive parameters include the averaged inlet mixture velocity and the inclination angle of gravity which does not affect greatly on this passive separation system.

CHAPTER 5:

CONCLUSIONS AND RECOMMENDATIONS

In petroleum industry, T-junctions are very common within pipe networks as they are commonly used to transport the components which are oil, gas and water prior to flow to the place of destination. It is important to understand the efficiency of the phase separation and the geometric effect of the T-junctions on the flow split in order to achieve a better separation performance for optimal operation of downstream components from the junction. This study is mainly focus on phase separation in T-junction with horizontal main arm and vertical side arm using methane gas and water as working fluids. Using the developed simulation model, the significance of associated parameters on two-phase separation efficiency in T-junction is studied. The diameter ratio, initial gas saturation, overall mass split ratio, averaged inlet mixture velocity and gas density are identified as the main factors affecting the fraction of gas taken off in T-junction. It is found that among these factors, the most influential factor is the overall mass split ratio followed by the initial gas saturation and diameter ratio of the T-junction. As a conclusion, application of a T-junction has the potential to be an alternative and economical partial phase separator for separation processes in the industries.

Since geometrical configuration plays an important role in phase separation, it would be interesting to examine different configurations of T-junction to determine the best selection criteria for a much wider range of flow conditions. Hence, future research can be done to study the effect of side arm inclination on the fraction of gas taken off. On top of that, the orientation of T-junction such as the vertical main arm with horizontal side arm should be considered as well to look into the effect of inclination angle of gravity in order to achieve the desired separation targets. Besides, more studies can be done using crude oil as one of the working fluids to examine the phase separation efficiency and flow splitting behavior in T-junction. Lastly, temperature effect on two-phase separation efficiency can also be analyzed in order to obtain more accurate and

complete results.

REFERENCES

- [1] Azzopardi, B. J. (1999, October). The effect of side arm diameter on phase split at T-junctions. In *SPE Annual Technical Conference and Exhibition*.
- [2] Azzopardi, B. J., Colman, D. A., & Nicholson, D. (2002). Plant application of a T-junction as a partial phase separator. *Chemical Engineering Research and Design*, **80**(1): 87-96.
- [3] Azzopardi, B. J., & Rea, S. (1999). Modelling the split of horizontal annular flow at a T-junction. *Chemical Engineering Research and Design*, **77**(8):713-720.
- [4] Azzopardi, B. J., & Rea, S. (2000, October). Phase separation using a simple T-junction. In *SPE Annual Technical Conference and Exhibition*.
- [5] Baker, G. (2003). *Separation and control of gas-liquid flows at horizontal T-junctions*. PhD dissertation, University of Nottingham, UK.
- [6] Barnea, D., Shoham, O., & Taitel, Y. (1980). Flow pattern characterization in two phase flow by electrical conductance probe. *International Journal of Multiphase Flow*, **6**(5):387-397.
- [7] Barnea, D. and Taitel, Y. (1985), Flow pattern transition in two-phase gas-liquid flow, *Encyclopedia of Fluid Mechanics*, Gulf Publishing, Houston, Texas, 16: 403-474.
- [8] Das, G., Das, P. K., & Azzopardi, B. J. (2005). The split of stratified gas-liquid flow at a small diameter T-junction. *International journal of multiphase flow*, **31**(4):514-528.
- [9] Davis, M. R., & Functamasan, B. (1990). Two-phase flow through pipe branch junctions. *International Journal of Multiphase Flow*, **16**(5): 799-817.
- [10] Hong, K. C. (1978). Two-phase flow splitting at a pipe tee. *Journal of Petroleum Technology*, **30**(2): 290-296.
- [11] Hwang, S. T., Soliman, H. M., & Lahey Jr, R. T. (1988). Phase separation in dividing two-phase flows. *International journal of multiphase flow*, **14**(4): 439-458.
- [12] Issa, R. I., & Oliveira, P. J. (1994). Numerical prediction of phase separation in two-phase flow through T-junctions. *Computers & fluids*, **23**(2): 347-372.
- [13] Jeanmeure, L. F. C. (2001), "Electrical capacitance tomography for flow control", *Ph. D. thesis*, University of Manchester Institute of Science and Technology, Manchester, England.

- [14] Jones Jr, O. C., & Zuber, N. (1975). The interrelation between void fraction fluctuations and flow patterns in two-phase flow. *International Journal of Multiphase Flow*, **2**(3): 273-306.
- [15] LIU, Y., & LI, W. (2011). Numerical Simulation On Two Phase Bubbly Flow Split In A Branching T-junction. *International Journal of Air-Conditioning and Refrigeration*, **19**(04): 253-262.
- [16] Mak, C. Y., Omebere-Iyari, N. K., & Azzopardi, B. J. (2006). The split of vertical two-phase flow at a small diameter T-junction. *Chemical engineering science*, **61**(19): 6261-6272.
- [17] Margaris, D. P. (2007). T-junction separation modeling in gas–liquid two-phase flow. *Chemical Engineering and Processing: Process Intensification*, **46**(2): 150-158.
- [18] Marti, S., & Shoham, O. (1997). A unified model for stratified-wavy two-phase flow splitting at a reduced T-junction with an inclined branch arm. *International journal of multiphase flow*, **23**(4): 725-748.
- [19] Nematollahi, M., & Khonsha, B. (2012). Comparison of T-junction flow pattern of water and sodium for different geometries of power plant piping systems. *Annals of Nuclear Energy*, **39**(1): 83-93.
- [20] Oliveira, P. J. D. S. P. (1992). *Computer modeling of multidimensional multiphase flow and application to T-junctions* (Doctoral dissertation, Imperial College London (University of London)).
- [21] Penmatcha, V. R., Ashton, P. J., & Shoham, O. (1996). Two-phase stratified flow splitting at a T-jun. *International journal of multiphase flow*, **22**(6): 1105-1122.
- [22] Peng, F. (1994). A study of dividing steam-water flow in T-junctions: Experiments and analyses.
- [23] Puspitasari, D., & Indarto, P. (2012). Liquid-Liquid Separation in T-Junction with Orientation Vertical Up Branch: Variation of Diameter Ratio in 15 mm Bend Radius. *International Journal of Research and Reviews in Mechatronic Design and Simulation (IJRRMDS)*, **2**(3).
- [24] Roberts, P. A., Azzopardi, B. J., & Hibberd, S. (1997). The split of horizontal annular flow at a T-junction. *Chemical engineering science*, **52**(20), 3441-345

- [25] Smith, A. V. (1975). Fast response multi-beam x-ray absorption technique for identifying phase distribution during steam water blow downs. *Journal of British Nuclear Engineering Society*, **14**(20): 227-235
- [26] Stacey, T., Azzopardi, B. J., & Conte, G. (2000). The split of annular two-phase flow at a small diameter T-junction. *International journal of multiphase flow*, **26**(5): 845-856.
- [27] Suzanne, G., & Choi, J. (1998, May). Two-Phase Flow Splitting at Side-Branching Tees. In *SPE Western Regional Meeting*.
- [28] Wolden, A. (2012). *Evaluation of Split Ratio for Plug Flow at a Meso-Scale T-Junction* (Doctoral dissertation, Norwegian University of Science and Technology).
- [29] Wren, E., Baker, G., Azzopardi, B. J., & Jones, R. (2005). Slug flow in small diameter pipes and T-junctions. *Experimental thermal and fluid science*, **29**(8), 893-899.
- [30] Wren, E. M. K. (2001). *Geometric effects on phase split at a large diameter T-junction* Doctoral dissertation, University of Nottingham.